

UNCLASSIFIED

AD NUMBER

AD907456

LIMITATION CHANGES

TO:

Approved for public release; distribution is unlimited.

FROM:

Distribution authorized to U.S. Gov't. agencies only; Test and Evaluation; 15 JAN 1973. Other requests shall be referred to Air Force Weapons Laboratory, Attn: AFWL (DEZ), Kirtland AFB, NM 87117.

AUTHORITY

AFWL per DTIC form 55 dtd 31 Apr 1986

THIS PAGE IS UNCLASSIFIED

AD 907 456

AUTHORITY:

AFWL etc

30 APR 86



AFWL-TR-72-183

AFWL-TR
72-183

AD907456

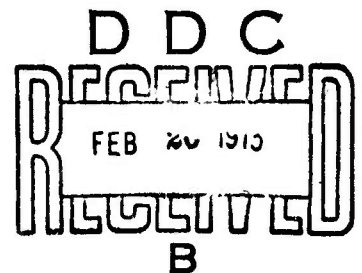


BOMB CRATER DAMAGE TO RUNWAYS

Peter S. Westine
Southwest Research Institute

TECHNICAL REPORT NO. AFWL-TR-72-183

February 1973



AIR FORCE WEAPONS LABORATORY
Air Force Systems Command
Kirtland Air Force Base
New Mexico

Distribution limited to U.S. Government agencies only because of test and evaluation (15 Jan 73). Other requests for this document must be referred to AFWL (JEZ), Kirtland AFB, NM.

AIR FORCE WEAPONS LABORATORY
Air Force Systems Command
Kirtland Air Force Base
New Mexico 87117

When US Government drawings, specifications, or other data are used for any purpose other than a definitely related Government procurement operation, the Government thereby incurs no responsibility nor any obligation whatsoever, and the fact that the Government may have formulated, furnished, or in any way supplied the said drawings, specifications, or other data, is not to be regarded by implication or otherwise, as in any manner licensing the holder or any other person or corporation, or conveying any rights or permission to manufacture, use, or sell any patented invention that may in any way be related thereto.

DO NOT RETURN THIS COPY. RETAIN OR DESTROY.

AFWL-TR-72-183

BOMB CRATER DAMAGE TO RUNWAYS

Peter S. Westine

Southwest Research Institute

TECHNICAL REPORT NO. AFWL-TR-72-183

**Distribution limited to U. S. Government agencies
only because of test and evaluation (15 Jan 73).
Other requests for this document must be referred
to AFWL (DEZ), Kirtland AFB, NM 87117.**

FOREWORD

This report was prepared by Southwest Research Institute, San Antonio, Texas, under Contract F29601-72-C-0053. The research was performed under Program Element 63723F, Project 683M.

Inclusive dates of research were February 1972 through November 1972. The report was submitted 8 December 1972 by the Air Force Weapons Laboratory Project Officer, Major Charles H. Neubauer (DEZ).

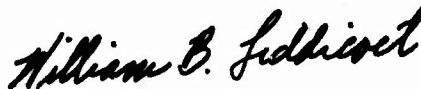
This technical report has been reviewed and is approved.



CHARLES H. NEUBAUER
Major, USAF
Project Officer



OREN G. STROM
Lt Colonel, USAF
Chief, Aerospace Facilities
Branch



WILLIAM B. LIDDICOET
Colonel, USAF
Chief, Civil Engineering Research
Division

ABSTRACT

(Distribution Limitation Statement B)

A similitude analysis is conducted and procedures are presented for using model tests to determine the extent of bomb crater damage to rigid runways. The radius, depth, and volume of true craters, as well as the extent of concrete cracking, can all be determined; however, different methods to scale the energy release are required, dependent upon a crater or camouflet being formed. Experimental test data using energy releases ranging from 5 grams to 589 pounds (750-pound bomb) of C-4 are used to demonstrate the validity of this model analysis. In addition, empirical equations have been curve-fitted to the pi terms and can be used for predicting mode of response, true crater size, and extent of concrete cracking.

TABLE OF CONTENTS

<u>Section</u>		<u>Page</u>
I.	INTRODUCTION	1
II.	NOMENCLATURE	4
III.	SOURCES FOR TEST DATA	9
IV.	MODEL ANALYSIS	19
V.	EVALUATION OF MODEL ANALYSIS	30
	Mode of Response	30
	Cratering Mode	34
	Camouflet Mode	48
VI.	FABRICATING MODELS	64
VII.	RECOMMENDATIONS FOR FUTURE EXPERIMENTS	70
VIII.	SUMMARY	74
	References	79

LIST OF FIGURES

<u>Figure</u>	<u>Title</u>	<u>Page</u>
1	Modes of Response and Nomenclature	5
2	Mode of Response	31
3	Normalized Surface Crater Radius In Cratering Mode	35
4	Normalized Crater Depth in Cratering Mode	36
5	Normalized Soil Crater Volume in Cratering Mode	37
6	Normalized Soil Plus Concrete Crater Volumes in Cratering Mode	38
7	Normalized True Crater Radius Without Pavement	42
8	Normalized True Crater Depth Without Pavement	43
9	Normalized True Crater Volume Without Pavement	44
10	Normalized Radius of Concrete Cracking in Cratering Mode	46
11	Normalized Maximum Crater Radius in Camouflet Mode	51
12	Normalized True Crater Depth in Camouflet Mode	52
13	Normalized Soil Plus Concrete Crater Volume in Camouflet Mode	53
14	Normalized Camouflet Radius Without Pavement	56

LIST OF FIGURES (cont'd)

<u>Figure</u>	<u>Title</u>	<u>Page</u>
15	Normalized Camouflet Volume Without Pavement	57
16	Normalized Surface Crater Radius in Camouflet Mode	59
17	Normalized Radius of Concrete Cracking in Camouflet Mode	62

LIST OF TABLES

<u>Table</u>	<u>Title</u>	<u>Page</u>
I	Fort Sumner Soil Properties	10
II	Hays, Kansas Soil Properties	12
III	Charge Sizes and Energy Release	15
IV	List of Symbols Used in Graphical Comparisons	16
V	List of Parameters	24
VI	Pi Terms - Obtained by Solving Relative to ρ_s , c, and d	25
VII	Pi Terms - Used in all Evaluations	26
VIII	Standard Deviation Crater Size in Cratering Mode	41
IX	Standard Deviation Crater Size in Camouflet Mode	54
X	Scale Factors for Model Cratering Experiments	69

SECTION I

INTRODUCTION

Whenever a bomb penetrates a runway or a charge is detonated beneath a paved surface, the resulting explosion creates a crater and cracks the pavement at large distances beyond the crater. The crater may be a large cavity which is open to the atmosphere, in which case we say the response has been in the cratering mode, or it may remain covered, in which case we say the response has been in the camouflet mode. Irrespective of the mode of response, rapid repairs require a knowledge of crater size and extent of concrete cracking.

Various researchers have concerned themselves with the somewhat analogous problem of predicting apparent crater size from buried explosive sources. Unlike these earlier studies, concerned largely with explosive excavation, we are not interested in apparent crater size. True crater size is a much more meaningful measure of damage to us. The debris which accumulates in the crater of a bomb-damaged runway may have to be removed, at least compacted, before repairs can commence. In addition, if one wishes to repair runways, the extent of concrete cracking is of extreme interest. Although procedures exist for estimating apparent crater size essentially no accurate procedures have been

developed for estimating true crater size. The initial intent of this study was to review the bomb cratering data that presently exist and determine if model tests could be conducted as a means for obtaining additional data inexpensively. We not only determined how models should be tested but also devised empirical methods for estimating true crater size and the extent of concrete cracking. Test data in a University of New Mexico report ^{(1)*} on charges ranging in size from 5.0 grams to 589 pounds of C-4 appear to confirm the applicability of any empirical equations.

Section II of this report deals with nomenclature. What is meant by modes of failure and more exact definitions of response parameters are presented in greater detail so that all readers and the author have common concepts whenever various terms are used. To evaluate this model analysis, experimental true crater data and pavement cracking data were required. Section III describes all test sites used by others (we performed no experimental tests ourselves) and indicates how any scaled graph should read so the test site, the pavement thickness, and the weight of charge is known at a glance for any data point. Section IV presents a detailed model analysis. Assumptions are enumerated and their implications discussed in detail.

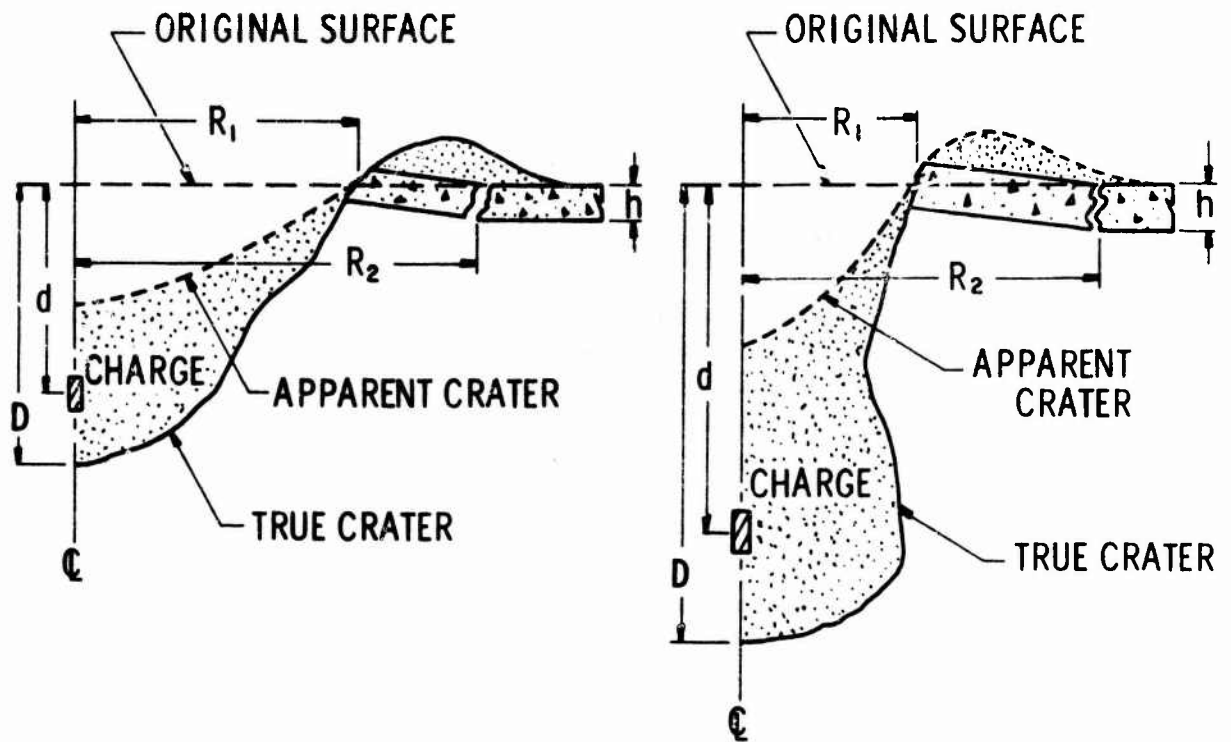
* Superscript numbers in parentheses refer to references at the end of this report.

An evaluation of this model analysis is presented in Section V. Section VI contains a description of how model tests should be scaled in the cratering and in the camouflet modes. Under certain conditions which are illustrated in Section VI, models cannot be used to simulate prototype response because the mode of response will change from cratering in the prototype to camouflet in the model. In Section VII a list of five recommendations for future experiments is presented. We recommend obtaining additional data to establish the line separating the cratering and camouflet modes over a wider range in initial conditions, collecting additional data over a wider range of charge weights in the camouflet mode, performing some model experiments to study the influence of concrete strength on surface related phenomena in both response modes, measuring the seismic velocity of soil at the various test sites, and perhaps performing some model tests of cratering from bomb detonations inside the pavement. A summary concludes this report and is presented in Section VIII.

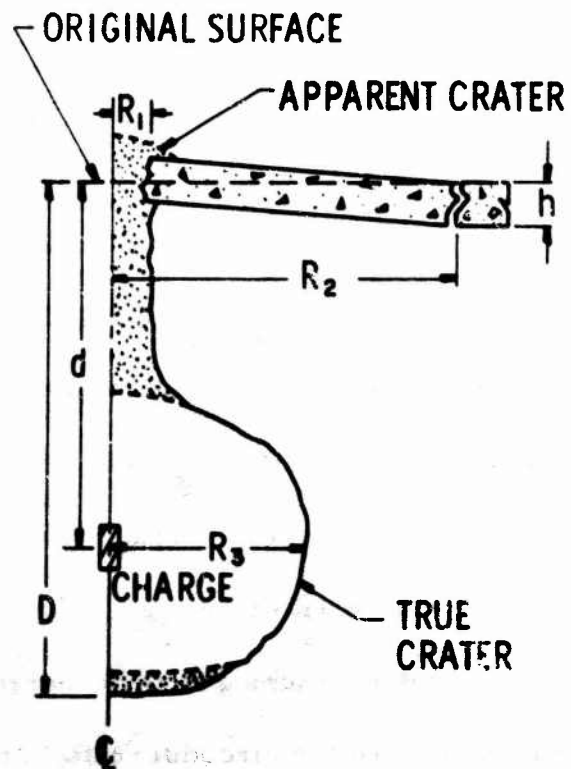
SECTION II

NOMENCLATURE

Before beginning this model analysis, or any analysis, the meanings of certain expressions must be clarified. Figure 1 and this discussion are presented to illustrate what we mean when certain terms are used. Whenever an explosive charge is detonated beneath the ground, a cavity or void is formed within the soil. If the energy release is relatively close to the surface, the cavity or void vents to the atmosphere and a crater is formed. Large amounts of ejecta are flung upwards and outwards if the cavity vents to the atmosphere. Some of this ejecta falls back into the cavity, whereas other amounts of it settle on the lip of the crater. Because large quantities of ejecta settle into the cavity, two different craters can be discussed; the apparent crater formed by the surface of the ejecta and the true crater formed by the crater boundaries without regard to the ejecta. Illustrations shown graphically in Figure 1 depict the differences in true and apparent craters. In this study, we are concerned with true crater dimensions only since those who repair bombed runways may have to remove the very loosely compacted ejecta before filling any void. In Reference 1 (which is the source for much of the experimental data used in this study), Kvammen, Pichumani and Dick treat craters which



CRATERING MODES



CAMOUFLET MODE

3676

Figure 1. Modes of Response and Nomenclature

vent or are open to the atmosphere as two separate and distinct modes of response dependent upon whether the true craters are somewhat hemispherical or cylindrical in shape. Although in Figure 1 we show cross sections of both types of craters discussed by Kvammen, Pichumani and Dick, we make no distinction between experimental results yielding either hemispherical or cylindrical true craters. In this report, any void venting to the atmosphere as in the top two illustrations in Figure 1 is said to have responded in the cratering mode.

If, on the other hand, the energy release is relatively deep within the ground, the cavity or void is created without any appreciable venting to the atmosphere. This mode of response as shown in Figure 1 is termed the camouflet mode. Very little ejecta is thrown into the air in the camouflet mode. A large spherical void is formed beneath the surface of the soil. Because physical phenomena, which are insignificant in determining true crater size in the cratering mode, become important in the camouflet mode, we study cratering and camouflet response as separate problems.

The responses of interest in either the cratering or camouflet modes are associated with true crater dimensions and the extent of circumferential cracking in the concrete. Long radial cracks extend way beyond the circumferential cracks in a damaged concrete pavement; however, it is the area of concrete covered

by both radial and circumferential cracks that require immediate repair. Kvammen, Pichumani, and Dick in Reference 1 present bomb cratering damage to runway experimental data through the use of six parameters. Because we rely so heavily on their compilation of data in this study, we use these six measures of response as defined in Reference 1 and as described below.

- (1) True Crater Depth (D) - Depth from the bottom of the true crater to the top of the original concrete surface.
- (2) Surface Crater Radius (R_1) - The average radius of the crater at the top of the original concrete surface. This average is calculated by taking the square root of the area at the crater surface divided by pi.
- (3) Radius of Concrete Cracking (R_2) - The concrete cracks beyond the surface crater radius. An average radius of circumferential cracking was calculated by taking the square root of the area enclosed by circumferential cracking in concrete divided by pi.
- (4) Maximum Crater Radius (R_3) - Maximum radius of true crater at any depth. For the cratering mode of response R_3 usually

equals R_1 . This parameter has more meaning in the camouflaged mode of response where the maximum radius occurs far below the surface of the soil.

- (5) True Soil Crater Volume (V_1) - Volume of the soil crater from the bottom of the concrete slab to the true crater walls.
- (6) Soil and Concrete Crater Volume (V_2) - Volume of concrete ejecta plus V_1 . The volume of the crater from the top of the slab to the true crater walls.

Other parameters used in this study are inputs rather than responses. They include the density of soil ρ_s , the density of concrete ρ_c , the ultimate strength of the concrete ρ_{ult} , the seismic wave velocity through the soil c , the acceleration of gravity g , the depth of burial for the explosive charge d , and the equivalent energy release W . Depth of burial is always measured from the top of the original concrete surface to the c. g. of the explosive source. Because different chemical explosives can be used as an energy source, we always consider the energy release W as an equivalent weight relative to an explosive called C-4. We use the energy of explosion as our criterion for relating explosive sources. The energy of explosion ⁽²⁾ for C-4 equals 1165 calories/gram.

SECTION III

SOURCES FOR TEST DATA

The data used for all evaluations of bomb crater damage to runways came from a single source by Kvammen, Pichumani, and Dick⁽¹⁾. This report contains a compilation of experimental test data from pavement cratering studies. Primarily all of the data in their report came from several different series of experiments at one of three different locations. Various experiments at these three different locations furnish us with enough data for evaluating the effects of charge weight, soil type, and pavement thickness on bomb crater damage to runways.

The Fort Sumner test site, located in Southeastern New Mexico, consisted of a 75-foot wide by 1,800-foot long by 7-inches thick concrete slab overlying a silty sand medium. Blowcount, dry density, moisture content, specific gravity, and the Atterberg limits were obtained at five different test boring locations and three different trench sites. Table I from Reference 1 gives an indication of soil conditions at Fort Sumner by showing the log for one of the bore holes. Additional soil details should be obtained from Appendix I in Reference 1. No base or subbase underlies the 7-inches of paving at Fort Sumner. The concrete was poured directly onto the soil; a runway paving technique typical of old World War II

Table I

FORT SUMNER SOIL PROPERTIES

Depth, ft	Unified Classification	Description	γ_d , pcf	g	LL	PI	w, %
Station S16							
1							
2							
3	SC	Clayey Sand	101.16	2.66	21	9	16.0
4							
5	SM	Silty Sand	104.62	2.67	16	2	8.5
6							
7							
8	SM	Silty Sand	104.67	2.69	SNP		9.5
9							
10	SP-SM	Sand w/Silt	121.14	2.66	SNP		4.5
11							
12	SW-SM	Gravelly Sand w/Silt	110.27	2.66	SNP		3.0
13							
14	CH	Fat Clays	114.34	2.67	59	36	24.0

vintage airfields. Because of this paving technique, the thickness of the concrete was approximately 7 inches with significant variations in thickness occurring. Most of the concrete pads were 20-foot long by 10-foot wide; however a few were 20-foot long by 15-foot wide. The average compressive strength of the concrete at Fort Sumner was 10,400 psi. Additional concrete test data for Fort Sumner may also be obtained from Appendix I in Reference 1.

The Hays, Kansas, test site consisted of a 150-foot wide by 5,600-foot long strip of concrete overlying a clay soil. Concrete thickness ranged from 11-inches for the center pads to 8-inches for the outlying pads. With the exception of blow count, the same soil properties were measured at Hays as at Fort Sumner. One of the boring logs, as presented in Reference 1, is shown in Table II to give an indication of soil conditions at Hays, Kansas. A wider variation in soil properties does exist at Hays than at Fort Sumner. No gravel base course underlies the paving at Hays either. Each concrete pad at Hays was approximately 20-foot long by 12.5-foot wide. The average compressive strength of the concrete at Hays was 10,100 psi, almost identical to the compressive strength for the concrete at Fort Sumner. Additional soil and concrete information about the Hays test site may be obtained from Appendix II in Reference 1.

Table II

HAYS, KANSAS SOIL PROPERTIES

Depth, ft	Unified Classification	Description	γ_d , pcf	G	LL	PI	w , %
Station 18+70							
1	CH	Darl Brown Clay	95.60	2.68	71	45	28.0
2	CH	Gray Brown Clay	102.60	2.69	54	32	23.0
3							
4							
5							
6	CH	Light Brown Clay	97.70	2.70	60	37	28.0
7							
8							
9	CL	Light Silty Clay	108.90	2.67	32	13	15.5
10							
11							
12							
13	CL	Light Silty Clay w/Large Proportions of Caliche	115.80	2.67	43	26	16.5
14							

In addition to the Fort Sumner and Hays cratering experiments, the University of New Mexico generated extra cratering data in a series of what they termed prototype and model tests⁽¹⁾. Only data from two prototype tests are included in Reference 1. These tests were conducted on a 14-inch thick concrete slab which has been spread over a 6-inch thick gravel base. Under the concrete and gravel was a 6-foot thick clay subgrade. The prototype pavement was divided by joints into 25-foot by 25-foot panels. No information concerning prototype concrete strength is given in Reference 1, and essentially no information about soil or gravel base properties.

The series of ten University of New Mexico model experiments is described in greater detail than the prototype experiments. In the model tests, a 2.75-inch thick concrete slab was poured over a 1.25-inch gravel base. Under the concrete and gravel lay a 15-inch thick layer of clay. The model pavement was divided by joints into panels 4 feet 10 inches square. The average compressive strength of the model concrete was 3705 psi which is considerably lower than the average compressive strengths for the Fort Sumner and Hays airfields. Density and moisture contents were reported for the model soils; these averaged 112.0 lb/ft³ and 11.0%, respectively.

The vast majority of the data used in an evolution of our modeling laws comes from the Fort Sumner and Hays Test sites. These data are supplemented by a few University of New Mexico prototype and model experiments. Different sizes of explosive charge were used at various test sites; 5-pound C-4, 15-pound C-4, and 25-pound C-4 charges were placed at various depths under 7.0-inch thick concrete at Fort Sumner, 8.0-inch thick concrete at Hays, and 11.0-inch thick concrete at Hays. In addition, 250-pound (MK-81), 500-pound (MK-82), and 750-pound (M-117) bombs were placed at various depths under 11.0 inch thick concrete at Hays only. The two prototype University of New Mexico experiments used 1.5 pound C-4 charges and the ten model experiments used various size C-4 charges ranging from 5.0 grams to 17.5 grams. Table III gives an indication of charge dimensions and the equivalent energy release. This writer believes that the three different types of bombs carried Tritonal, a very energetic chemical explosive with an energy of explosion of $1770 \text{ calories/gram}^2$. Because C-4 is a much less energetic explosive, an energy of explosion of $1165 \text{ calories/gram}^2$, the actual weight of explosive in each bomb was multiplied by 1.52 ($1770/1165$) to obtain an equivalent C-4 energy release. The influence of bomb casing on the energy release is assumed to be insignificant.

Table III

CHARGE SIZES AND ENERGY RELEASES

<u>Explosive Source</u>	<u>Diameter of Explosive Source(in.)</u>	<u>Length to Diameter Ratio</u>	<u>Actual Weight of Explosive(lb)</u>	<u>Equivalent C-4 Energy Release</u>
5.0 lbs C-4	4.0	1.87	5.0	5
15.0 lbs C-4	6.0	1.66	15.0	15
25.0 lbs C-4	7.0	1.75	25.0	25
250 lb Bomb	9.0	5.48	101.5	154
500 lb Bomb	10.75	6.	192.5	292
750 lb Bomb	16.1	3.17	387.0	589

Notice also that the bombs are many diameters longer than the C-4 explosive charges. We are of the opinion that this length to diameter aspect ratio has an insignificant influence on true crater dimensions and the extent of concrete cracking; nevertheless, we mention this observation for the sake of completeness. All depths of burial were measured and will be used in our analysis relative to the c. g. of the explosive source. No geometric charge dimensions were given for the University of New Mexico prototype and model explosive sources; hence, this information cannot be included in Table III. The prototype and model experiments did report their charge weights, and the explosive used in these experiments was C-4.

Throughout the many graphical comparisons which are about to be made for evaluations of modeling laws, we use experimental test data from the various test sites and numerous different sizes of explosive charges. To tell for any given data point what was the charge size, what was the thickness of the overlying concrete, and how large was the energy release, we had to devise a systematic procedure for presenting the test data from Reference 1. Table IV illustrates this procedure graphically. Basically the procedure involves use of shading to denote the test site and concrete thickness, and use of symbol shape to denote magnitude of the energy release.

Table IV

LIST OF SYMBOLS USED IN GRAPHICAL COMPARISONS

TEST SITE	FORT SUMNER	HAYS KANSAS	HAYS KANSAS	U. OF NEW MEXICO	U. OF NEW MEXICO
WEIGHT EXPLOSIVE CHARGE / CONCRETE THICKNESS (in.)	7.0	8.0	11.0	2.75	14.0
5.0 to 17.5 gms C-4				X	
1.5 lb C-4					+
5.0 lb C-4	△	△	△		
15.0 lb C-4	◇	◇	◇		
25.0 lb C-4	□	■	■		
250.0 lb BOMB			●		
500.0 lb BOMB			●		
750.0 lb BOMB			●		

The white symbols are for data points taken at Fort Sumner, the black symbols are for data points taken at Hays with 11.0 inches of concrete as overburden, and the speckled or gray figures are for data points taken at Hays with 8.0 inches of concrete as overburden. All model tests irrespective of the size of the energy release are shown by the symbol X, and the two prototype 1.5-pound experiments are denoted by a plus sign +. The larger the energy release, the more sides are given to a symbol (a circle is assumed to have an infinite number of sides). Table IV shows that the energy release increases as the symbols change from triangles, to diamonds, to squares, to pentagons, to hexagons, and finally to circles. All graphs in this report for evaluating model approaches to experimental bomb crater damage to runways use the system of symbols presented in Table IV.

Most experiments report true crater radius at the surface R_1 , average radius of concrete cracking R_2 , maximum true crater radius at any depth R_3 , depth of true crater D , volume of true crater without including concrete V_1 , and volume of true crater and damaged concrete V_2 . In a few experiments, some of the parameters are not reported so we cannot include them. For example, all of the bomb data report surface effects R_1 and R_2 ; however, we cannot include in this study D , V_1 , V_2 and R_3 for some of the bomb experiments because some craters were never excavated. Reference 1 also does not report radii R_1 and R_3 in the prototype

University of New Mexico tests. We use all data whenever it is reported. In making evaluations using the University of New Mexico prototype and model test data, we assume that the thickness of the pavement is that of the concrete slab, and that the gravel base is part of the soil media.

In some of our graphical comparisons, we use cratering data for experiments with no paving for confinement. These data come from a compendium compiled at Waterways Experiment Station ⁽³⁾, and are used to demonstrate that under certain conditions the scaled thickness of pavement and scaled concrete strength are insignificant parameters in determining certain true crater dimensions. We do not use different symbols or shadings to denote test site location or magnitude of the energy release for data from Reference 3, cratering without confinement from paving; nevertheless, these true cratering data come from tests in clay, sand, moist loess, and wet silt, and include equivalent energy releases of 0.25, 0.50, 1.0, 8.0, 25, 27, 54, 64, 256, 320, 3560, 40,000, and 320,000 pounds of TNT. Tables 1 and 2 in the Appendices of Reference 3, and in Reference 3 itself, should be studied by those seeking additional information about these data.

SECTION IV

MODEL ANALYSIS

Any model analysis reflects the definition of the problem. Physical phenomena that are not considered cannot appear in the resulting pi terms. In this study we exercise our opinion and engineering judgment to list parameters which we feel may be significant. A problem such as this one to define true crater dimensions and predict radius of concrete cracking is very difficult and subject to differences in professional opinion. In defining this problem, we attempt to indicate what assumptions are being made. Subsequent nondimensional plots are presented to illustrate the degree to which this model analysis is valid and to provide physical insight into the significance of the analysis.

The parameters which we consider include the total energy release in the buried explosive charge W and the depth of burial from the top surface of the concrete d . We do not include parameters defining the geometry of the explosive source, nor do we list parameters for studying the explosive process and the propagation of shocks within the explosive. Two main reasons exist for deleting these details from the analysis. First, we wish to keep our list of parameters as small as is practically possible. Second, we are not interested in the intensity of pressures and other lo-

calized details in the vicinity of the charge; we are interested in gross overall response on a much larger scale, such as true crater dimensions. By listing only W and d as input parameters related to the explosive source, we are assuming that the energy release is instantaneous relative to cratering times and originates from a source whose size is insignificant.

The major difficulty in this problem is the selection of appropriate parameters for characterizing soil behavior. Out of necessity we assume that the soil is homogeneous to an infinite depth, isotropic, and a single phase medium. Admittedly pore air and pore water pressures within the granular structure of the soil influence shear strength; however, this process is so poorly understood in soil dynamics that we cannot expect to reflect complex behavior in an applied problem seeking numerical values. We characterize the properties of soil using three parameters: the density of the media ρ_s , the seismic velocity of the soil c , and the acceleration of gravity g . These three parameters are selected because this investigator has had some success in applying them to a related problem ⁽⁴⁾, the apparent crater dimensions caused by the detonation of a buried explosive charge. Selecting only three parameters for characterizing soil does permit the ground to behave as a fluid close to the charge and as a solid at greater standoff

distance. Inertial effects are incorporated into the analysis through the density ρ_s . Gravitational effects are included because the acceleration of gravity g is listed, as well as ρ_s . The seismic velocity parameter c when considered in combination with ρ_s represents the soil's constitutive strength. The product $\rho_s c^2$ is a measure of the compressibility of the ground. It takes on finite numerical values for all soil types and never equals zero. Other parameters (unconfined compressive strength, cone indexes, etc.) which might be selected as a measure of constitutive strength often are numerically either infinite or zero for certain extremes in soil conditions. These parameters are unacceptable measures of constitutive strength as they lead to indeterminate solutions even when we are physically aware that craters do form. By selecting only three soil parameters, we represent the maximum number of three physical phenomena (gravitational, inertial, and constitutive effects) with the absolute minimum number of parameters.

We do not include strain rate effects in this analysis by listing a rate of strain parameter because we believe these effects are insignificant. Certainly all cratering events are at high rates of strain, but the parameters ρ_s and c are measures of constitutive behavior at quite high rates of strain also. Provided constitutive strength is not appreciably modified by changes in the rates of strain between the smallest and the largest charges, this

assumption is acceptable. Usually many orders of magnitude change in rate of strain are required to appreciably modify constitutive properties. Going in charge weight from 1 pound to 1000 pounds while holding everything else constant approximately changes the rate of strain by only one order of magnitude, an insignificant amount for appreciably modifying constitutive properties.

Because the ground is covered by slabs of concrete, we must list parameters for defining concrete properties. We assume that the concrete has little or no reinforcing steel, and that it extends to infinity in the plane of the earth's surface. Although we list no steel reinforcing properties in this analysis, we present our views about simulating pavements with large amounts of reinforcing after we analyze test results and discuss how to construct model airfield cratering experiments. The concrete pavement is of thickness h and has inertial properties represented by the density parameter ρ_c and constitutive strength represented by the ultimate compressive strength of the concrete σ_{ult} . We assume strain rate effects are insignificant in the concrete as in the soil, and that the ultimate tensile strength of concrete, toughness, and/or other strength characteristics may be thought of as constant ratios relative to the ultimate compressive stress σ_{ult} .

So far in this analysis, we have characterized the explosive source, the soil, and the concrete pavement. Next we must decide

what responses are of interest. Each of these responses or results is a function of the input explosive, soil, and concrete parameters; they are not functions of one another. For any given experimental test, we would like to know whether the response will be in the cratering or the camouflet modes. Mode shape is a nondimensional parameter which we shall call "MODE". We would like to predict true crater size, what quantity of concrete becomes ejecta, and over how large a region the concrete is cracked. Because Kvammen, Pichumani, and Dick in Reference 1 report true crater depth D , surface crater R_1 , average radius of circumferential concrete cracking R_2 , maximum crater radius R_3 , true soil crater volume V_1 , and soil and concrete crater volumes V_2 , we use these six convenient dependent parameters as our response parameters. From these six parameters, one can estimate true crater size and the extent of damage to the pavement which requires repair.

Table V lists the eight independent input parameters, plus the seven dependent response parameters which we have just described, and presents their fundamental dimensions in the engineering system of force F , length L , and time T .

Table V

LIST OF PARAMETERS

Independent Input Parameters

<u>Symbol</u>	<u>Parameter</u>	<u>Fundamental Dimensions</u>
W	Energy Release in Explosive	FL
d	Depth of Explosive Burial	L
ρ_s	Density of Soil	FT^2/L^4
g	Acceleration of Gravity	L/T^2
c	Soil Seismic Velocity	L/T
ρ_c	Density of Concrete	FT^2/L^4
σ_{ult}	Ultimate Strength Concrete	F/L^2
h	Thickness of Concrete	L

Dependent Response Parameters

<u>Symbol</u>	<u>Parameter</u>	<u>Fundamental Dimensions</u>
MODE	Mode of Response	---
D	Depth of Crater	L
R_1	Surface Crater Radius	L
R_2	Radius of Concrete Cracking	L
R_3	Maximum Crater Radius	L
V_1	Soil Crater Volume	L^3
V_2	Concrete and Soil Volume	L^3

Because there are fifteen parameters and three fundamental dimensions, we can develop five independent pi terms and seven dependent response pi terms by applying the Buckingham Pi Theorem. The mathematics of obtaining these pi terms are straightforward and will not be repeated in this report; no new assumptions are introduced into this analysis because we go through the tedious algebra of obtaining these nondimensional ratios. If one solves for pi terms with respect to the parameters ρ_s , c , and d , he will obtain the pi terms shown in Table VI.

Table VI

PI TERMS - OBTAINED BY SOLVING RELATIVE TO ρ_s , c , and d

Independent Pi Terms

$$\begin{aligned} \pi_1 &= h/d \\ \pi_2 &= \rho_c / \rho_s \\ \pi_3 &= \sigma_{ult} / \rho_s c^2 \\ \pi_4 &= gd/c^2 \\ \pi_5 &= W / \rho_s c^2 d^3 \end{aligned}$$

Dependent Response Pi Terms

$$\begin{aligned} \pi_6 &= \text{MODE} \\ \pi_7 &= R_1/d \\ \pi_8 &= R_2/d \\ \pi_9 &= R_3/d \\ \pi_{10} &= D/d \\ \pi_{11} &= V_1/d^3 \\ \pi_{12} &= V_2/d^3 \end{aligned}$$

Pi terms may be multiplied or divided by one another to form new pi terms. They may be taken to any power. These manipulations are performed for the convenience of the investigator. Although the pi terms in Table VI are a perfectly acceptable set, this writer finds it convenient to rewrite pi term 4 as the ratio of energy release relative to the energy expended in overcoming gravitational effects rather than use it in its present format of gravitational effects relative to constitutive effects. Dividing pi term 5 by pi term 4 to obtain a new pi term 4, then taking the 1/4 root of the new pi term 4, 1/3 root of pi term 5, 1/3 root of pi term 11, and 1/3 root of pi term 12 yields the pi terms shown in Table VII. The pi terms shown in Table VII are used in all subsequent analyses.

Table VII

PI TERMS - USED IN ALL EVALUATIONS

Independent Pi Terms

$$\pi_1 = h/d$$

$$\pi_2 = \rho_c / \rho_s$$

$$\pi_3 = \sigma_{ult} / \rho_s c^2$$

$$\pi_4 = W^{1/4} / \rho_s^{1/4} g^{1/4} d$$

$$\pi_5 = W^{1/3} / \rho_s^{1/3} c^{2/3} d$$

Dependent Response Pi Terms

$$\pi_6 = \text{MODE}$$

$$\pi_7 = R_1/d$$

$$\pi_8 = R_2/d$$

$$\pi_9 = R_3/d$$

$$\pi_{10} = D/d$$

$$\pi_{11} = V_1^{1/3}/d$$

$$\pi_{12} = V_2^{1/3}/d$$

Provided that the parameters which we have listed as measures of concrete strength and soil strength are appropriate and provided that constitutive, inertial, and gravitational effects are the physical phenomena involved in the cratering event, Equation (1) for any of the response pi terms in Table VII is a prediction equation interrelating all variables in a bomb crater damage to runway analysis.

$$\pi_{\text{dependent parameter}} = f \left(\frac{h}{d}, \frac{\rho_c}{\rho_s}, \frac{\sigma_{\text{ult}}}{\rho_s c^2}, \frac{W^{1/4}}{\rho_s^{1/4} g^{1/4} d}, \frac{W^{1/3}}{\rho_s^{1/3} c^{2/3} d} \right) \quad (1)$$

This equation defines a six-parameter space of nondimensional products. It is much too large a space to empirically generate an entire solution for Equation (1) as presented. Fortunately, as a first-order approximation, certain parameters may be treated as constant, and, as a result, Equation (1) can be simplified.

We will treat ρ_c , ρ_s , g , c , and σ_{ult} as constants in subsequent analysis. The fact that the first three of these five parameters are essentially constant should disturb no one. Very little variation of less than +15% occurs in ρ_c , ρ_s , and g from experiment to experiment. The other two parameters, c and σ_{ult} , do have the capability for significant variation. Unfortunately seismic velocity c is not reported in the test data compiled in Reference 1. For most sands and clays, c will range from around 600 to 6000 fps. We will assume c is constant for the soils

used in Reference 1 because we cannot assign numerical values until this parameter is measured. Earlier work⁽⁴⁾ on an analogous problem, apparent crater size from buried explosive charges, indicates that treating c as a constant for various types of soil does not significantly modify apparent crater geometry.

For all practical purposes, σ_{ult} was a constant for most of the tests reported in Reference 1. At the Fort Sumner test site, the average ultimate compressive strength from twelve tests on concrete cylinders equaled 10,400 psi, and, at Hays, this same test on nine concrete cylinders gave σ_{ult} as 10,100 psi. The vast majority of all data was taken at Fort Sumner and Hays. In the University of New Mexico model experiments, the average concrete ultimate strength was 3705 psi, considerably lower than at Hays and Fort Sumner. The ultimate concrete strength is not reported in the two University of New Mexico prototype tests. We will assume σ_{ult} was a constant in all experimental tests, but, whenever model test results disagree with Fort Sumner and Hays results, one should consider if the cause of any disagreement could be low values of σ_{ult} .

If we assume ρ_c , ρ_s , g , c , and σ_{ult} are constants, we can treat these parameters as abstract numbers, and write a simplified, four-parameter version of Equation (1). Equation (2)

is this simplified version of Equation (1). Note that ρ_c / ρ_s and $\sigma_{ult} / \rho_s c^2$ disappear from Equation (1), because these terms are now invariant, and that two of the independent quotients in Equation (2) are now dimensional because portions of those pi terms have been treated as abstract numbers. Because $W^{1/4}/d$ and $W^{1/3}/d$ are now dimensional, we use W in equivalent pounds of C-4 and d in feet of burial.

$$\pi_{\text{dependent parameters}} = f \left(\frac{h}{d}, \frac{W^{1/4}}{d}, \frac{W^{1/3}}{d} \right) \quad (2)$$

Equation (2) with a few variations depending upon mode of response and response parameter being studied is used for evaluating this model analysis.

SECTION V

EVALUATION OF MODEL ANALYSIS

Mode of Response

Equation (2) indicates that the mode of response (cratering mode or camouflet mode) should be a function of normalized concrete thickness $\frac{h}{d}$ and two different normalized charge weights $\frac{W^{1/3}}{d}$ and $\frac{W^{1/4}}{d}$. Actually mode shape is very insensitive to normalized pavement thickness, so Equation (3) can be used instead of Equation (2) for predicting mode of response.

$$\text{MODE} = f_{\text{mode}} \left(\frac{W^{1/3}}{d}, \frac{W^{1/4}}{d} \right) \quad (3)$$

To prove that Equation (3) is appropriate, consider the experimental data presented in Figure 2. All data points shown in Figure 2 follow our standard convention for plotting data. In addition, either a vertical slash or a horizontal slash bisects each data point in Figure 2. If the slash is vertical on this plot of $2.0 + \log \frac{W^{1/3}}{d}$ versus $2.0 + \log \frac{W^{1/4}}{d}$, the response was in the cratering mode, and if the slash is horizontal, the response was in the camouflet mode. The number two was arbitrarily added to each data point because the writer did not care to have negative values for the logarithm of any normalized parameters. This manipulation only translates the X and Y axis in any plot; it does not modify conclusions. All logarithms in this figure and subse-

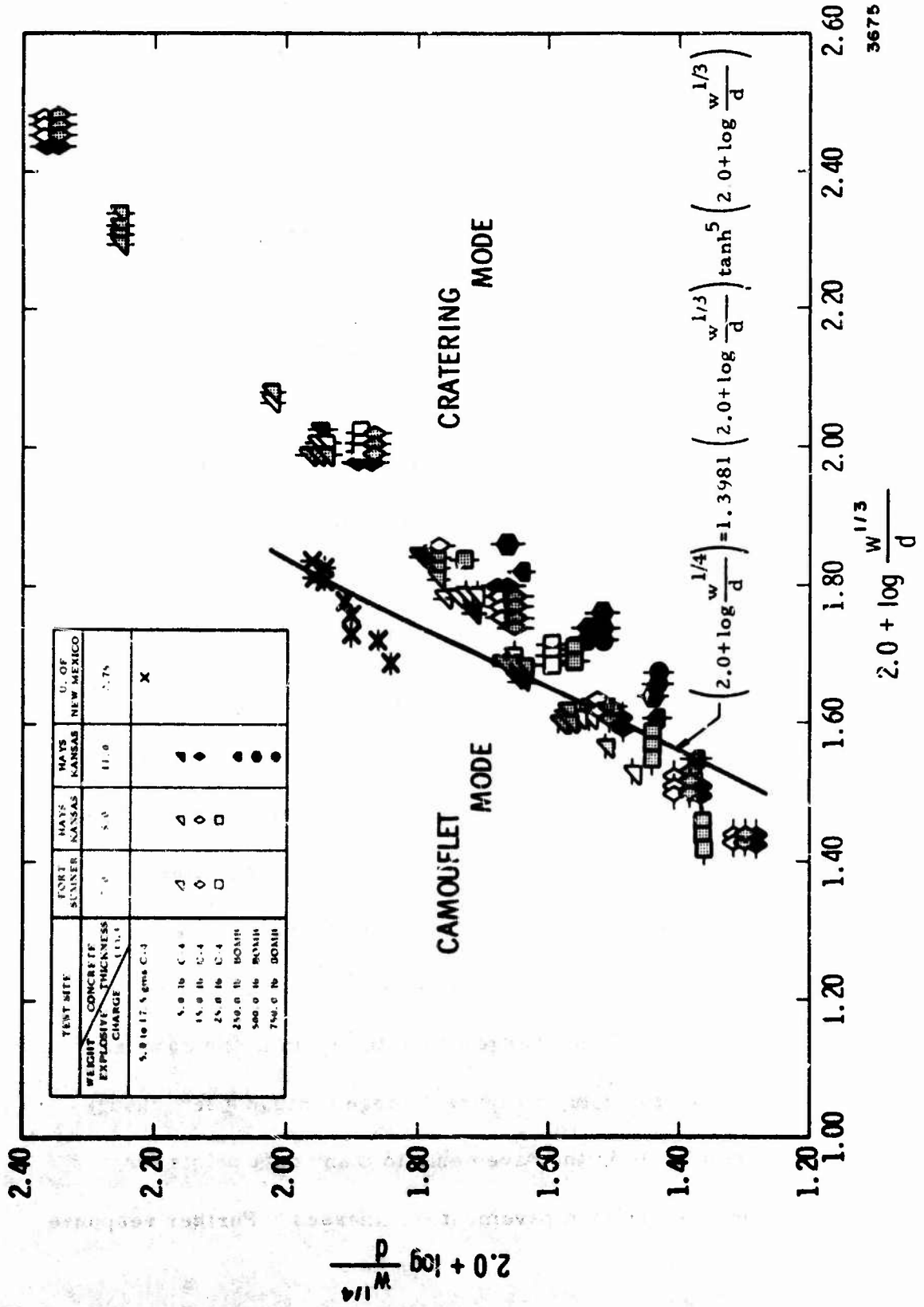


Figure 2. Mode of Response

quent figures are to the base ten. The charge weight W in Equation (3) and Figure 2 is in equivalent pounds of C-4, while the depth of burial d is in feet of burial.

Notice in Figure 2 that a curved line separates the data responding in the cratering mode from the data responding in the camouflet mode. If the data fall to the left and above this line, the response was in the camouflet mode, and, if the data fall below and to the right of this line, the response was in the cratering mode. A few data points have both a solid slash and a dashed slash; the mode for the response of these points is uncertain, but the mode represented by the solid slash is the more probable of the two modes. Essentially all data fall on the appropriate side of the line separating the two modes; only a few exceptions exist. These exceptions are close to the line, and one must remember that we are treating ρ_s , g , and especially c as abstract numbers in the parameters represented by the X and Y coordinates in Figure 2. The parameter $\frac{h}{d}$ for the data in Figure 2 ranges from a low of 0.06 to a high of 1.39. A value of $\frac{h}{d}$ greater than 1.0 means that the c. g. of the charge was actually up in the concrete pavement. Hence, the data in Figure 2 range through a few charges which were actually up in the pavement, to many data points for charges buried over sixteen pavement thicknesses. Further response

evaluations will reveal that responses in the cratering mode are independent of pavement thickness and that all responses except perhaps the surface effects (R_1/d and R_2/d) are independent of pavement thickness in the camouflet mode. If other responses are independent of pavement thickness, then intuitively one should feel that mode of response would be independent of pavement thickness.

The curve which we passed between the data points in Figure 2 has an equation given by:

$$(2.0 + \log \frac{W^{1/4}}{d}) = 1.3981 (2.0 + \log \frac{W^{1/3}}{d}) \tanh^5 (2.0 + \log \frac{W^{1/3}}{d}) \quad (4)$$

Equation (4) is a functional method of expressing Equation (3).

If after substituting for $W^{1/3}/d$ in Equation (4) the calculated value of $W^{1/4}/d$ is greater than the intended experimental value, then the response falls in the camouflet mode. Otherwise if the calculated value of $W^{1/4}/d$ is less than the intended experimental value, the response should fall in the cratering mode. Equation (4) is only valid for values of $2.0 + \log W^{1/3}/d$ from 1.50 to 1.85 because this equation is a curve-fit to a limited quantity of experimental data, all of which fall within a narrow band on a plot, as shown in Figure 2.

Either Figure 2 or Equation (4) may be used to predict mode of response. Mode of response is important because the

crater dimensions and extent of concrete cracking scale in different manners dependent upon whether the response is in the camouflet or cratering modes.

Cratering Mode

In the cratering mode, all true crater dimensions are independent of all independent normalized parameters in either Equations (1) or (2), except $W^{1/3}/d$. This observation means that the shape of the true crater depends upon neither gravitational effects nor the strength and inertial effects of the concrete pavements. In other words, the explosive energy release is so overpowering that the pavement provides insignificant confinement, and gravitational effects only influence the free fall of the ejecta, an event which could not possibly modify true crater dimensions.

To demonstrate that true crater dimensions are a function only of $W^{1/3}/d$ in the cratering mode, Figures 3 through 6 present, respectively, scaled plots of surface crater radius, crater depth, soil crater volume, and soil plus concrete crater volumes as functions of $W^{1/3}/d$. The data used in these figures come for all the Reference 1 test sites, and the explosive charges range from a few grams up through bombs. The parameter h/d varies from a low of 0.07 to a high of 1.39. Seven data points represent test conditions with the c. g. of the explosive source up in the concrete

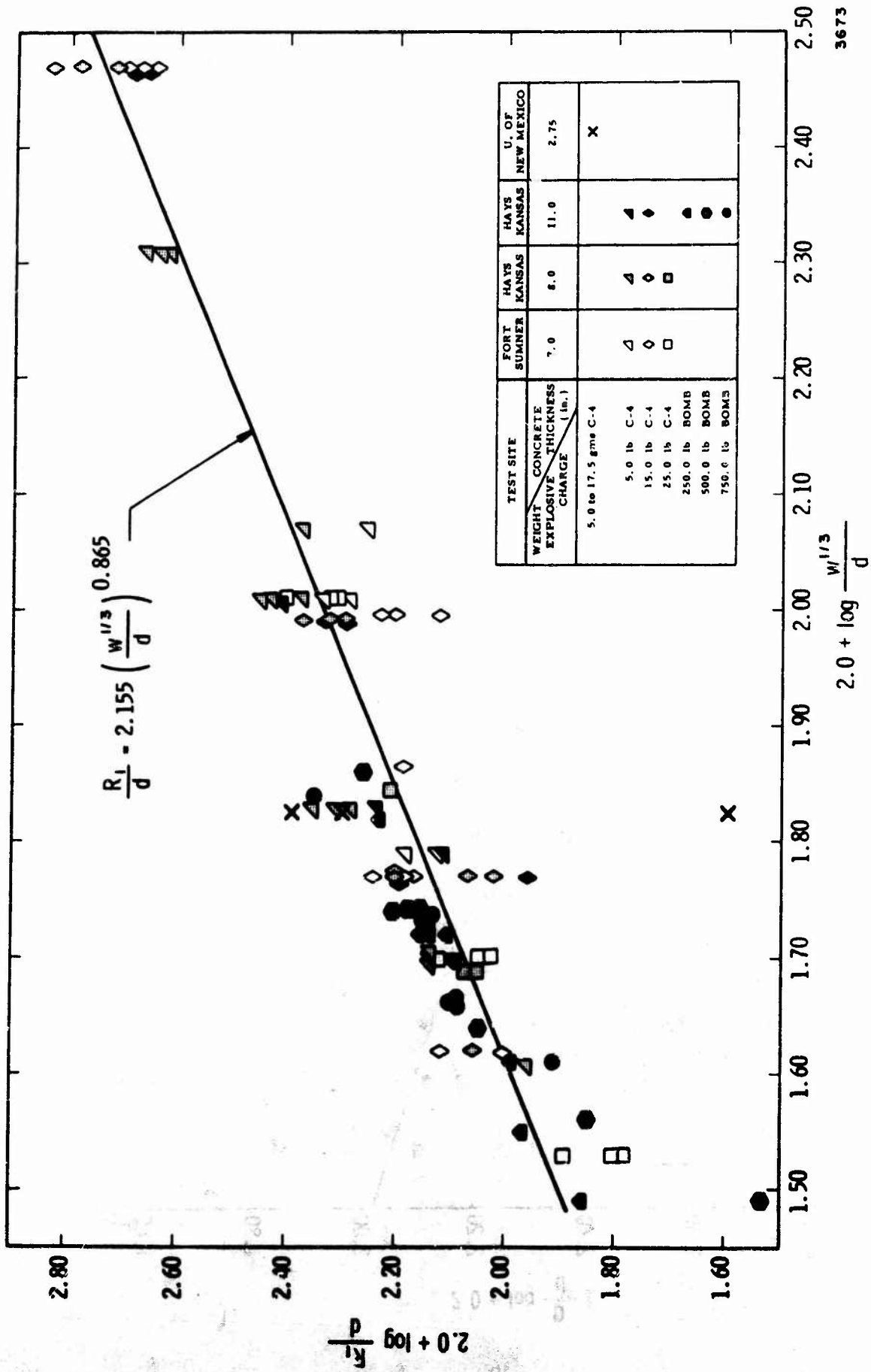


Figure 3. Normalized Surface Crater Radius in Cratering Mode

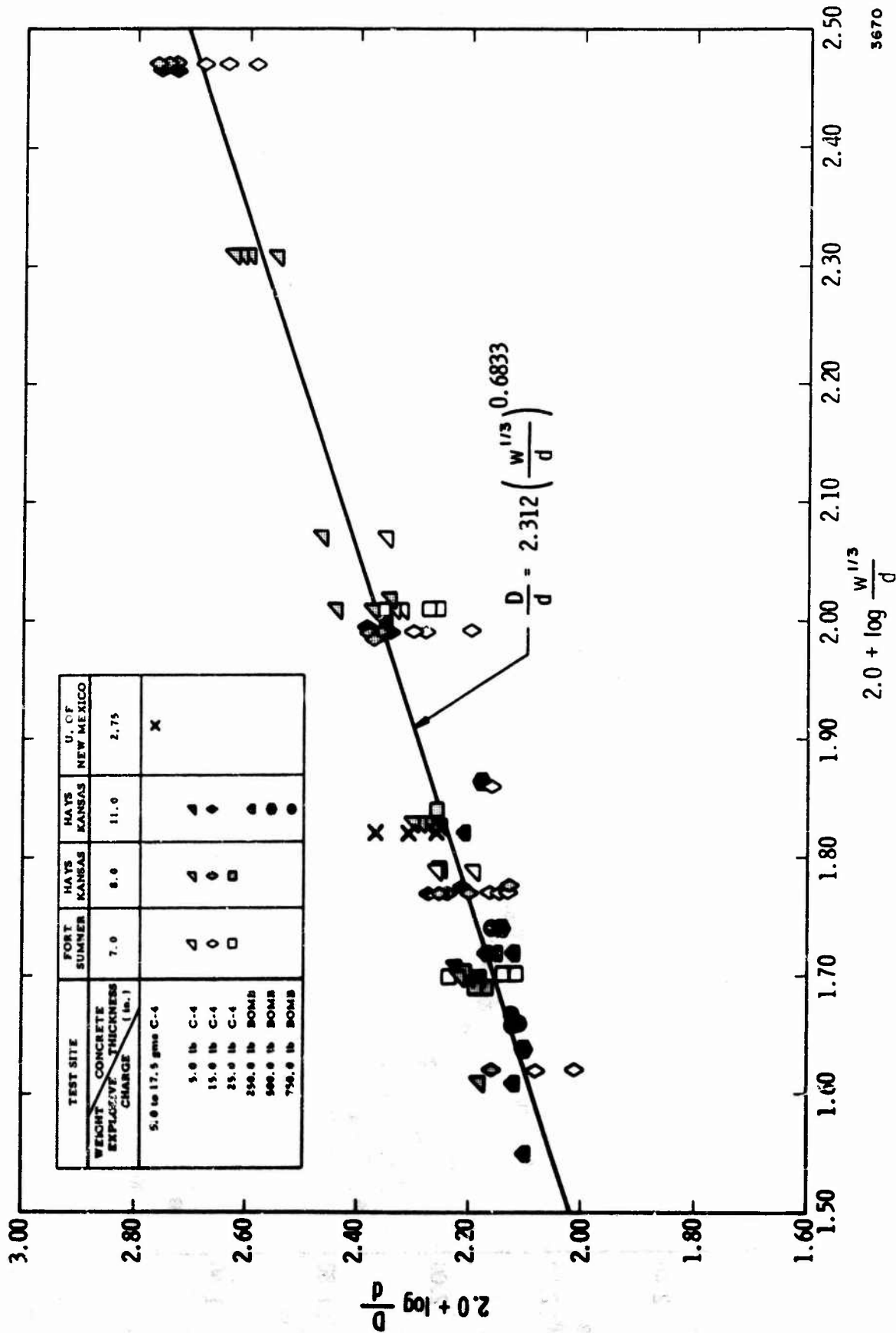


Figure 4. Normalized Crater Depth in Cratering Mode

3670

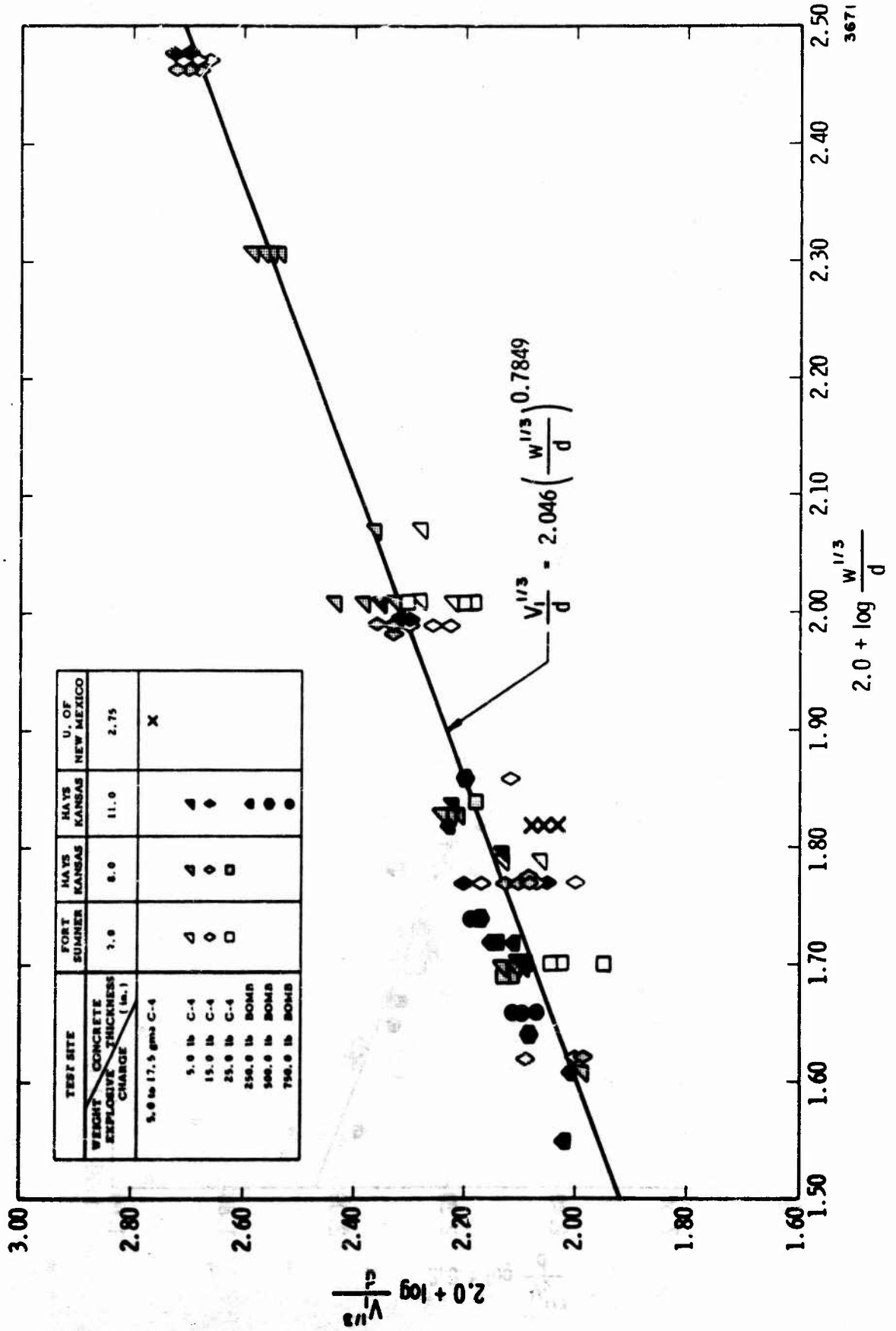


Figure 5. Normalized Soil Crater Volume in Cratering Mode

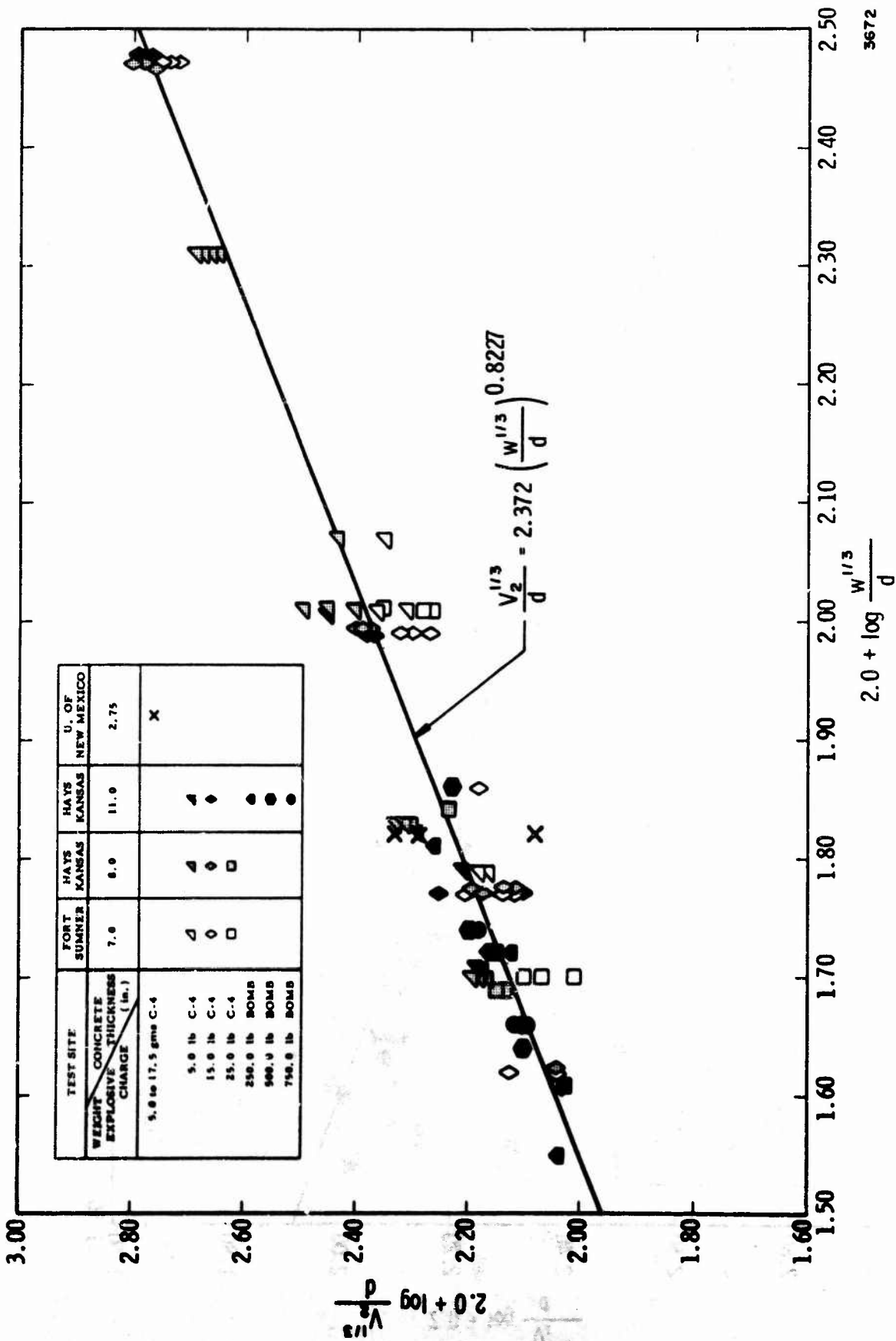


Figure 6. Normalized Soil Plus Concrete Crater Volumes in Cratering Mode

($1.00 \leq h/d \leq 1.39$). Figures 3 through 6 are log plots, with the number 2.0 arbitrarily added to the numerical value of a test result, so negative values would not occur when the logarithm was less than one. As in Figure 2, this manipulation shifts the X and Y axes, but does not modify conclusions. Some scatter occurs in the data presented in Figures 3 through 6; however, this observer feels that it is random rather than systematic. All logarithms have been taken to the base ten in these true crater dimension figures; therefore, a difference of two in test results is represented by a factor of approximately 0.3 in Figures 3 through 6 (logarithm of 2.0 equals 0.30103). The range for all the data in these figures is significantly less than a factor 2.0 in the response π term. Figure 3, R_1/d , has the largest scatter among any of the true crater figures, but this parameter should scatter more because relative to the other cratering response parameters R_1/d is poorly defined. Often the slope of the true crater near the surface asymptotically approaches the horizon; hence, different observers easily assign various numerical values to R_1 when they cannot tell exactly where a crater begins. The parameter R_3 has not been presented as a measure of crater size because in the vast majority of cases R_3 equals R_1 for responses in the cratering mode.

Straight lines have been least-square curve-fitted to the data in Figures 3 through 6. The equations to these lines which

functionally relate the response pi terms to $W^{1/3}/d$ are given by:

$$\frac{R_1}{d} = 2.155 \left(\frac{W^{1/3}}{d} \right)^{0.865} \quad (5)$$

$$\frac{D}{d} = 2.312 \left(\frac{W^{1/3}}{d} \right)^{0.6833} \quad (6)$$

$$\frac{V_1^{1/3}}{d} = 2.046 \left(\frac{W^{1/3}}{d} \right)^{0.7849} \quad (7)$$

$$\frac{V_2^{1/3}}{d} = 2.372 \left(\frac{W^{1/3}}{d} \right)^{0.8227} \quad (8)$$

In addition, standard deviations have been calculated by dividing theoretically predicted responses from Equations (5) through (8) into experimentally observed responses. This manipulation which yields new distributions about a mean of unity permits the computation of standard deviations for R_1/d , D/d , $V_1^{1/3}/d$, and $V_2^{1/3}/d$ about their respective predictive equation. Table VIII summarizes these results. As indicated in Table VIII, one standard deviation essentially equals 12% except for the less well conditioned R_1/d where it equals 20.4%. This observer believes these results are excellent. Further improvements in accuracy might be achieved if one had actual values of $\rho_s c^2$ to substitute into the independent pi term; however, practical problems would require some averaging procedure for obtaining an effective value

of $\rho_s c^2$ because of changes in $\rho_s c^2$ with depth. In the opinion of this writer, which presently cannot be substantiated with experimental data, variations of $\rho_s c^2$ with depth in real soil will prevent orders of magnitude improvements in accuracy.

Table VIII
STANDARD DEVIATION CRATER SIZE IN
CRATERING MODE

<u>Parameter</u>	<u>Standard Deviation</u>
R_1/d	20.4%
D/d	12.2%
$V_1^{1/3}/d$	12.7%
$V_2^{1/3}/d$	11.9%

As additional evidence that h/d is an insignificant parameter in the cratering mode, plots have been made from data in Reference 2 of true crater surface radius, true crater depth, and true crater volume without any pavement present to act as constraint. Figures 7, 8 and 9 which present these plots compare this unconstrained true crater data to the least-square curve-fit lines and the standard deviations about these lines from, respectively, Figure 3 for surface crater radius, Figure 4 for crater depth, and Figure 6 for soil and concrete volume. The airfield

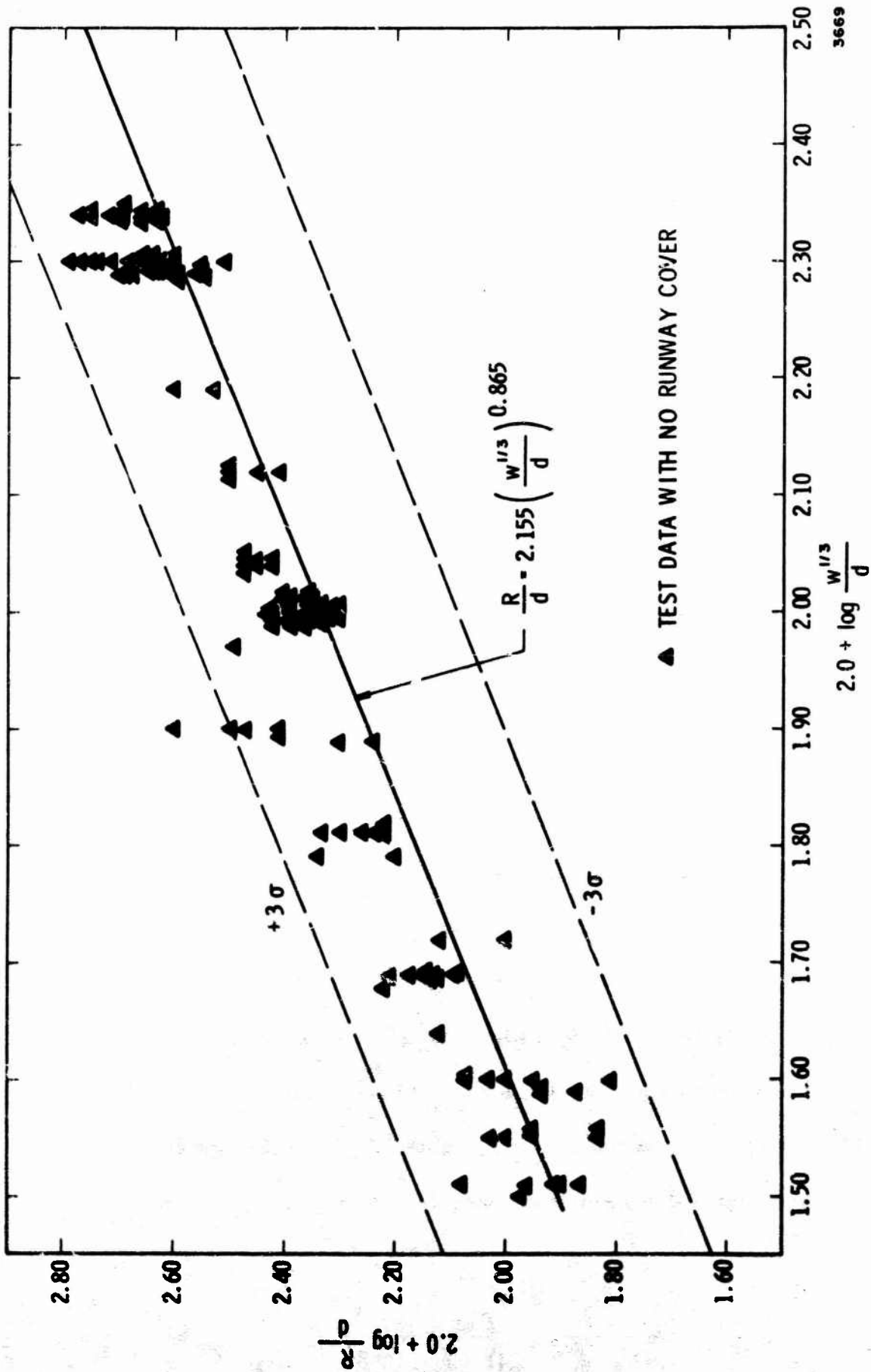


Figure 7. Normalized True Crater Radius Without Pavement

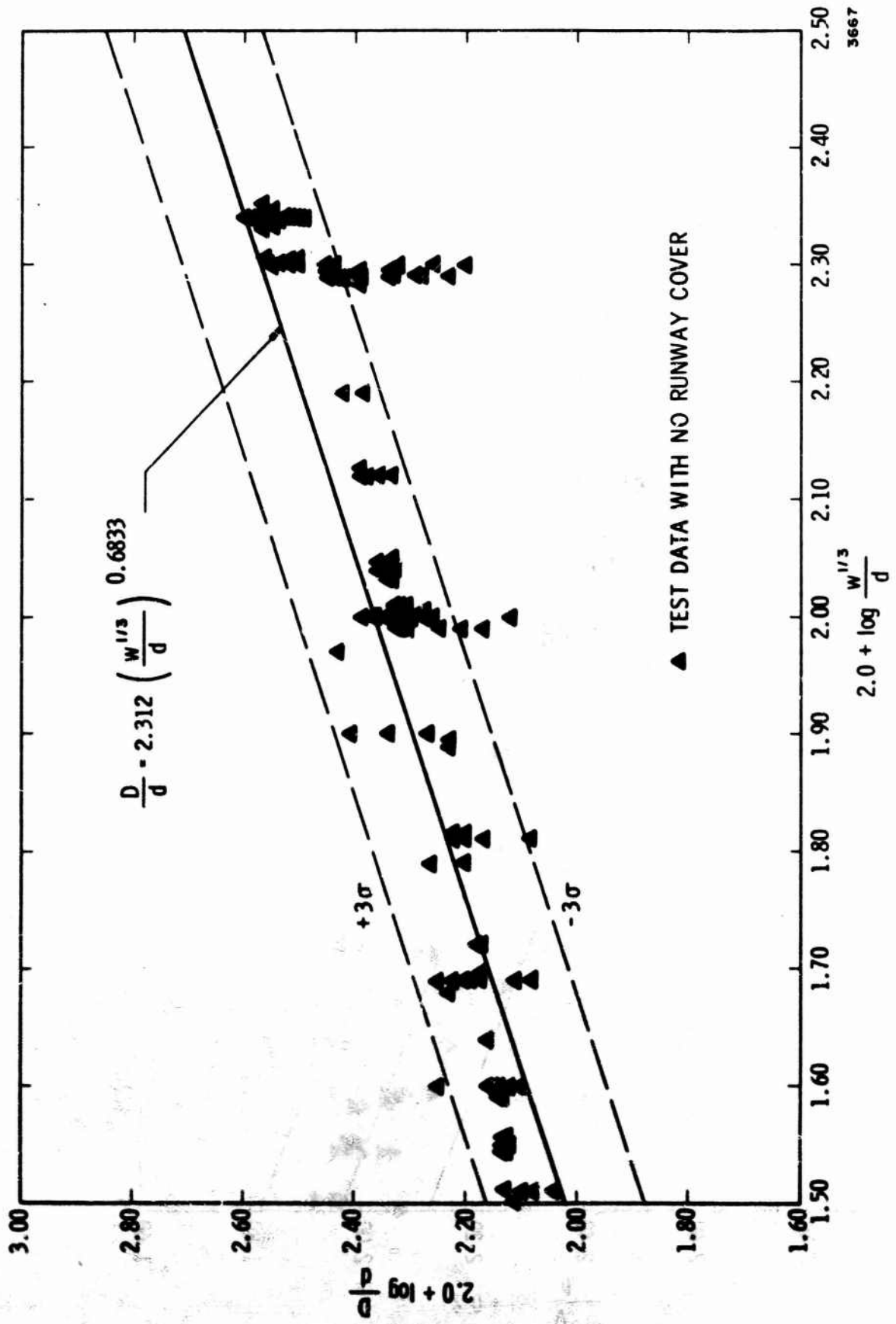


Figure 8. Normalized True Crater Depth Without Pavement

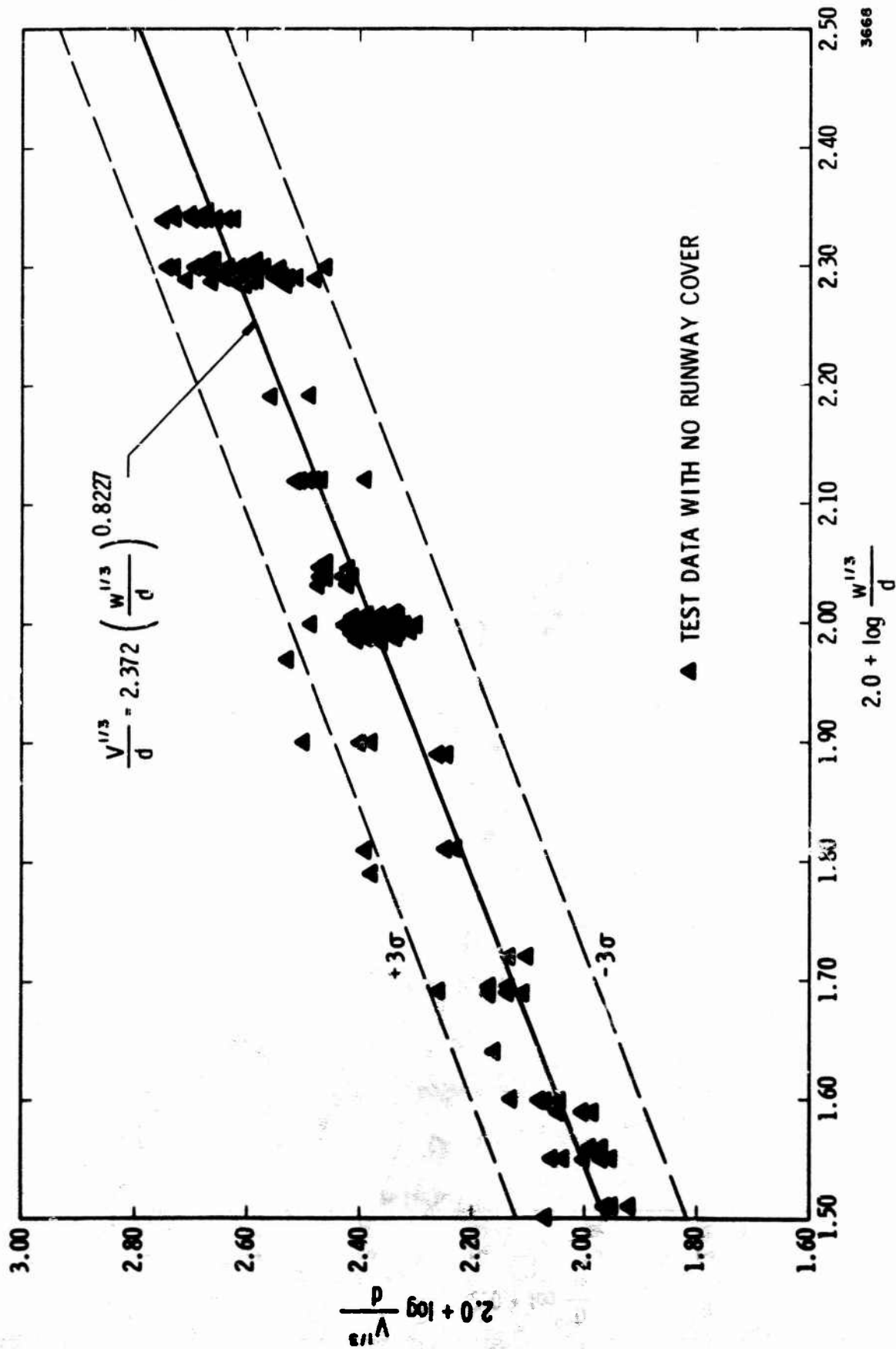
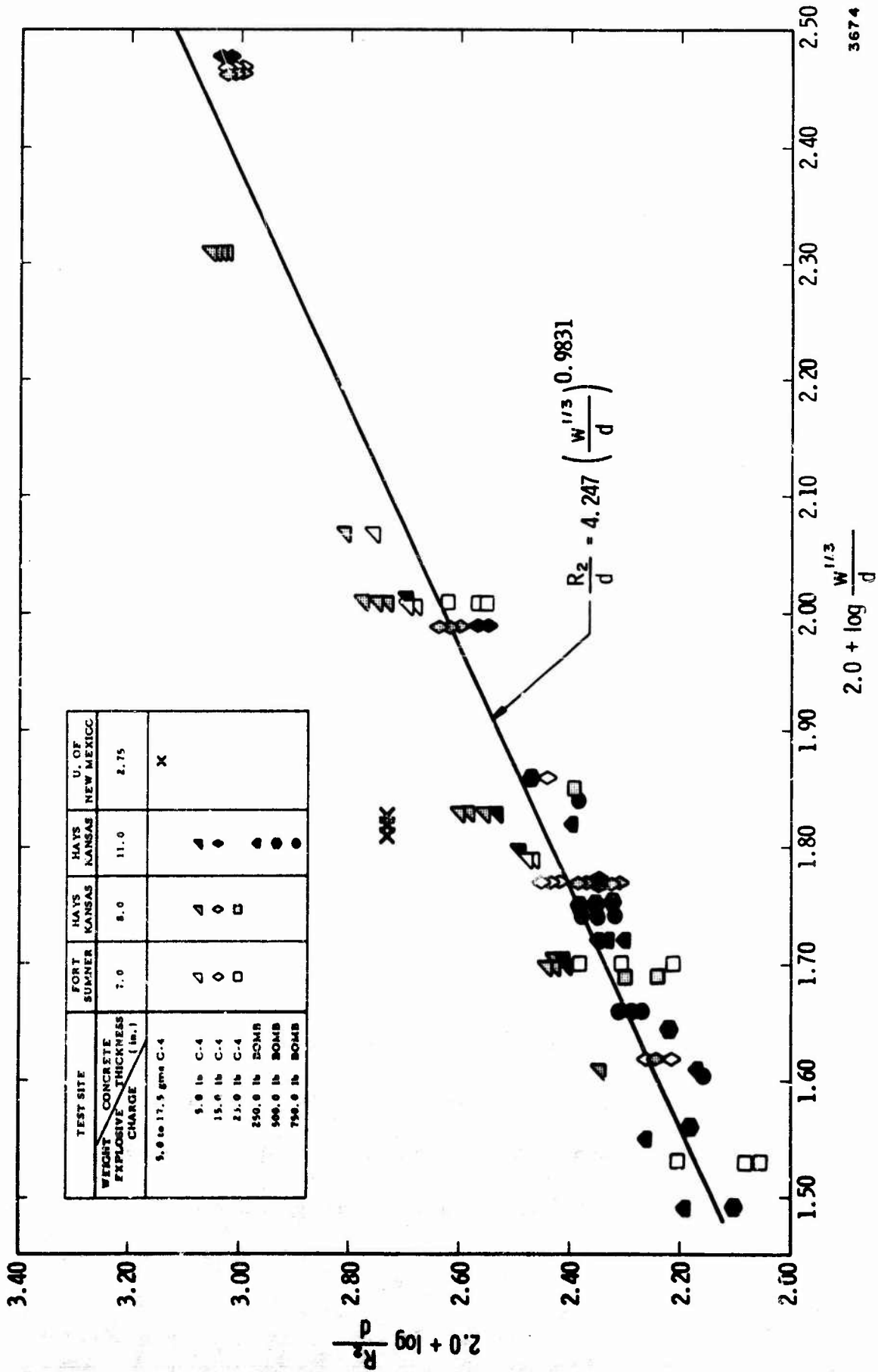


Figure 9. Normalized True Crater Volume Without Pavement

cratering experiments appear to predict cratering results for h/d equal to zero, especially when one considers the scatter in both runway cratering results as represented by the 3σ standard deviation bounds and in unconstrained craters as depicted by individual data points. Without the presence of pavement, surface crater radius is slightly larger, but crater depth is slightly shallower especially for shallow depths of burial than would be predicted with the presence of pavement. Crater volumes are essentially identical with or without the presence of pavement. These observations substantiate further that true crater dimensions are influenced only slightly in the cratering mode by normalized pavement thickness. If pavement thickness does not influence crater size, this observer does not believe that pavement strength, the pi term $\sigma_{ult} / \rho_s c^2$ will have any influence on true crater geometry. The parameter $\sigma_{ult} / \rho_s c^2$ equaled zero when no pavement was present and equaled some finite value in Reference 1 experiments; hence, true crater size should also be independent of this scaled parameter in the cratering mode.

So far, we have evaluated cratering parameters; we have not determined average radius of circumferential cracking in the concrete, a surface phenomenon which is influenced by normalized concrete strength, $\sigma_{ult} / \rho_s c^2$. Figure 10 presents $R_2 d$ as a



3674

Figure 10. Normalized Radius of Concrete Cracking in Cratering Mode

function of $W^{1/3}/d$ for all cratering mode data in Reference 1.

This figure indicates that normalized radius of concrete cracking is a function of $W^{1/3}/d$, is a function of $\sigma_{ult}/\rho_s c^2$, but is not a function of $\frac{h}{d}$. Most of the data in Figure 10 collapse into a unique function relating R_2/d to $W^{1/3}/d$. Many different values of h/d ranging from 0.07 to 1.39 are included in these data, even though separate plots are not being constructed for different values of h/d . Therefore, normalized radius of cracking is independent of h/d within the limits being studied in h/d . The three data points which depart the most from test results in Figure 10 are all for University of New Mexico model tests. In the model experiments, the average ultimate concrete strength equaled 3705 psi; whereas, in all other experiments, the average ultimate concrete strength was within a few hundred psi of 10,200 psi. Because the concrete strength was weaker in the model tests than in all other experiments, the concrete cracked a greater scaled distance in model experiments. Obviously the concrete cracks because of up-heave in the underlying soil. Up-heave of the soil is not greatly influenced by scaled pavement thickness or scaled pavement strength; however, a scaled amount of up-heave will crack a weak concrete, whereas a stronger concrete may resist cracking in the same scaled amount of up-heave.

A least-squares fit to the data in Figure 10 may be achieved

using a straight line. This equation is only valid for concretes with an ultimate strength of approximately 10,200 psi. The equation is:

$$\frac{R_2}{d} = 4.247 \left(\frac{W^{1/3}}{d} \right)^{0.9831} \quad \text{provided } \sigma_{\text{ult}} = 10,200 \text{ psi} \quad (9)$$

One standard deviation about this line equals 16.5% if the model data are excluded from the other data. Throughout this analysis, we ignore the presence of any reinforcing and the size of slabs. Obviously joints in slabs can arrest propagating cracks, and reinforcing can effectively create a stronger concrete, especially in tension. Considering that these quantities are not scaled from test to test, this observer is amazed to find one standard deviation is only 16.5%. One can scale reinforcing and slab dimensions if models are being made of a specific situation; however, handling these complications in devising a formula creates a much larger space, a space which would be too large to develop an entire solution using only experimental results.

Camouflet Mode

In the camouflet mode, experimental results will show that normalized true crater maximum radius R_3/d , true crater depth D/d , and soil plus concrete crater volume $V_2^{1/3}/d$ are all insensitive functions of h/d and $\sigma_{\text{ult}}/\rho_s c^2$, but their dimen-

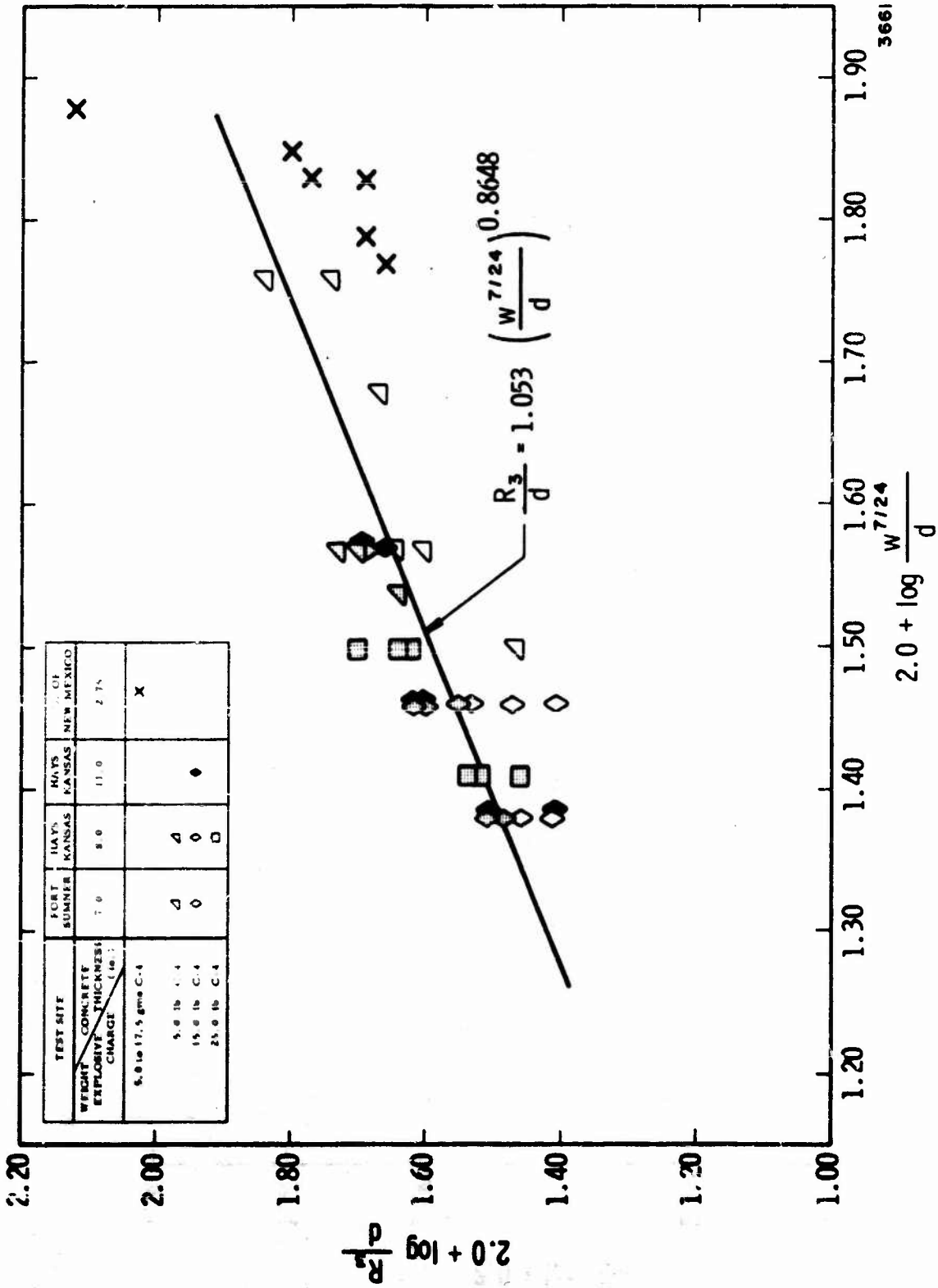
sions do depend upon both $W^{1/3}/d$ and $W^{1/4}/d$ in either Equation (1) or (2). This observation implies that the shape of the true crater in the camouflet mode depends on both gravitational effects and constitutive effects in the soil; however, the presence of a concrete pavement has only a minimal influence on crater size. If these ascertainment are correct, one cannot conduct a mode test in the camouflet mode that rigorously satisfies all pi terms unless troublesome and expensive test techniques are employed. Charge weight cannot simultaneously be scaled as both the cube of the depth of burial and the fourth power of the depth of burial. Fortunately, this apparent impass can be overcome by employing approximate techniques.

This writer in earlier studies⁽⁴⁾ indicated that apparent crater dimensions can be simulated if the normalized parameters $W^{1/3}/d$ and $W^{1/4}/d$ are combined through an empirical observation to form $\sqrt{(W^{1/3}/d) \cdot (W^{1/4}/d)}$ or $W^{7/24}/d$. In other words, we distort both pi terms by making one quantity too large and the other too small so compensating errors essentially provide correct results. Apparently this same empirical observation works with reasonable accuracy in scaling true crater dimensions within the camouflet mode.

To demonstrate that true crater dimensions are an approximate function of $W^{7/24}/d$ in the camouflet mode, Figures 11 through

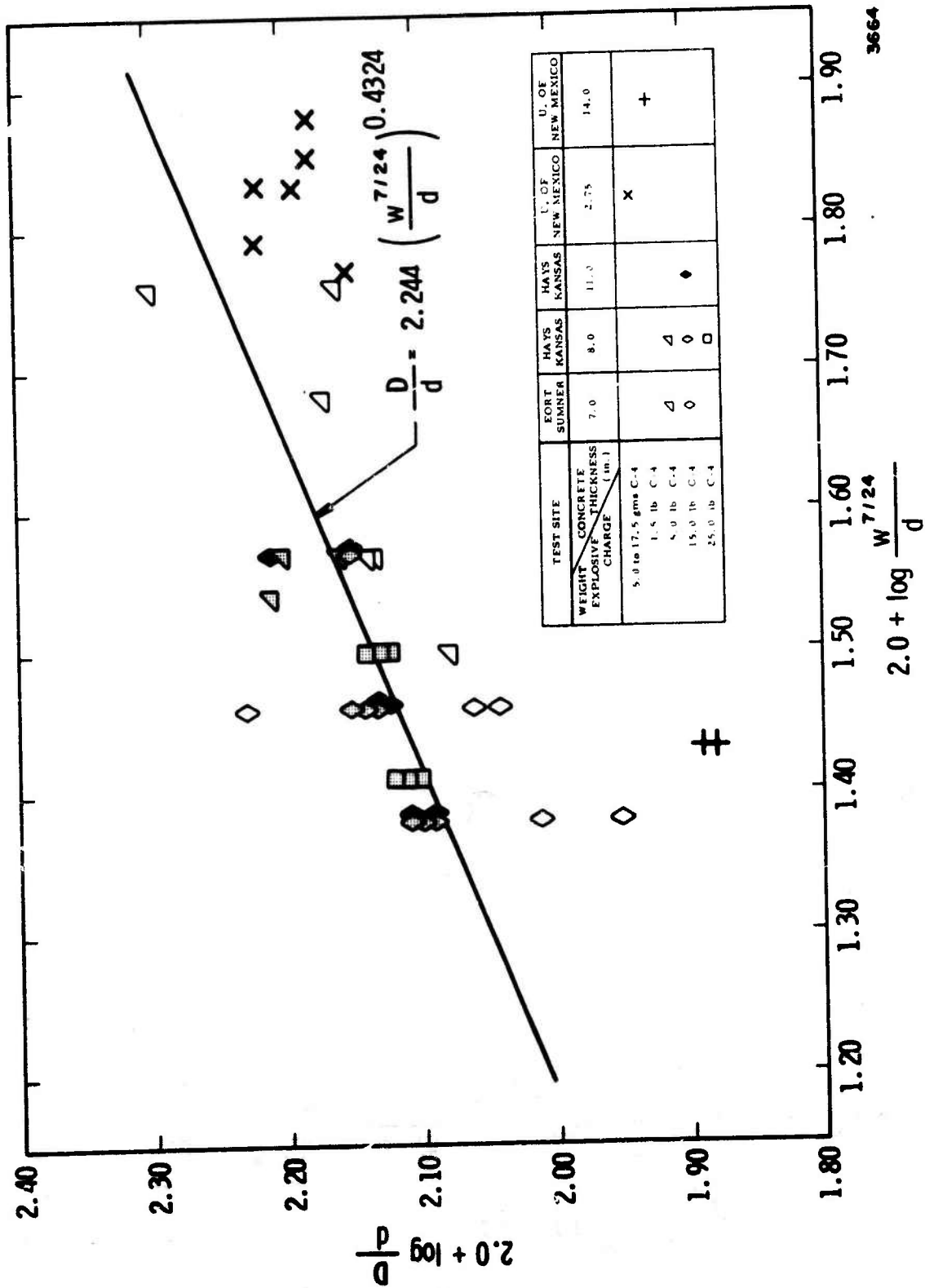
13 present, respectively, scaled plots of maximum crater radius R_3/d , crater depth D/d , and soil plus concrete crater volumes $\sqrt[3]{V_2}/d$ as functions of $W^{7/24}/d$. The data used in these figures comes from the Fort Sumner, Hays, and University of New Mexico model experiment test site. Unfortunately, no bomb cratering experiments were conducted in the camouflet mode; hence, air-field camouflet cratering experiments only cover a very small range in size of explosive charge, from 5 to 25 pounds of C-4. The parameter h/d does not range through as wide a variation in the camouflet mode as in the cratering mode because the camouflet mode is associated with relatively deep depths of burial. In the camouflet mode, h/d appears to be a secondary parameter in determining true crater size because the data in Figures 11 through 13 include values from 0.06 to 0.46 without being forced to consider h/d as significantly modifying results.

As in the cratering mode, straight lines have been least-squares curve-fitted to the Fort Sumner and Hays data in Figures 11 through 13. The University of New Mexico model experiment data are not included in determining the equation for this line, but these model experiment data points are shown graphically in Figures 11 through 13.



3661

Figure 11. Normalized Maximum Crater Radius in Camouflet Module



3664

Figure 12. Normalized True Crater Depth in Camouflet Mode

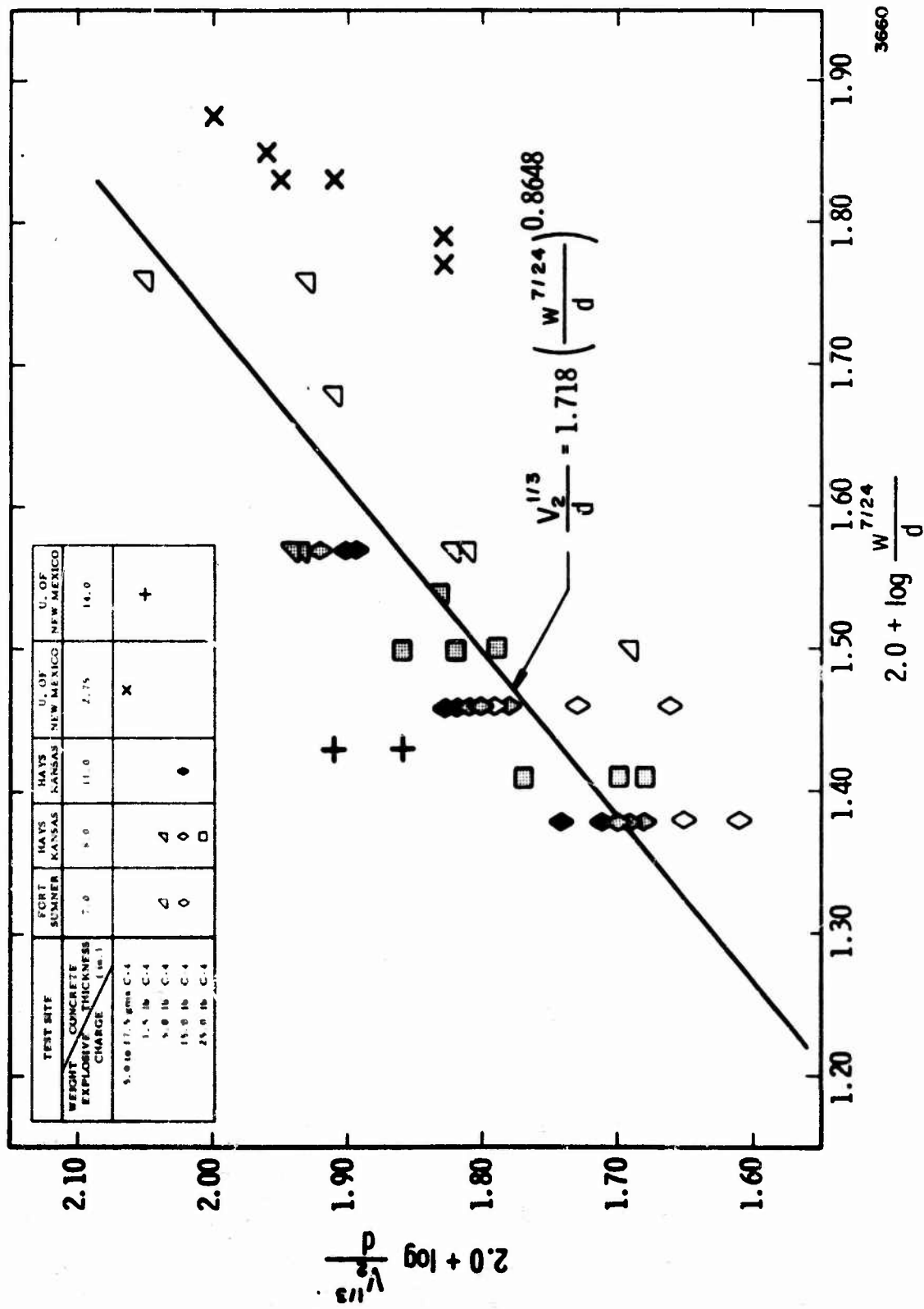


Figure 13. Normalized Soil Plus Concrete Crater Volume in Camouflet Mode

3660

The equation for these lines are given by:

$$\frac{R_3}{d} = 1.053 \left(\frac{W^{7/24}}{d} \right)^{0.8548} \quad (10)$$

$$\frac{D}{d} = 2.244 \left(\frac{W^{7/24}}{d} \right)^{0.4324} \quad (11)$$

$$\frac{V_2^{1/3}}{d} = 1.718 \left(\frac{W^{7/24}}{d} \right)^{0.8648} \quad (12)$$

Standard deviations were also calculated by dividing theoretically predicted responses from Equations (10) through (12) into experimentally observed responses as seen in Figures 11 through 13. Table IX presents the standard deviations for R_3/d , D/d , and $V_2^{1/3}/d$ in the camouflet mode as determined through this normalization manipulation for providing a large sample with a mean of unity.

Table IX
STANDARD DEVIATION OF CRATER SIZE
IN CAMOUFLET MODE

<u>Parameter</u>	<u>Standard Deviation</u>
R_3/d	13.5%
D/d	10.5%
$V_2^{1/3}/d$	11.9%

One standard deviation for any of the parameters in the camouflet mode essentially equals or is even a little less than the same standard deviation in the cratering mode, see Table VIII. Figures 11 through 13 may appear to give larger scatter than their counterparts in the cratering modes, Figures 3 through 5; however, the scale to which they are plotted is greatly enlarged relative to the scales presented in the cratering mode. To some degree, the Fort Sumner (open symbols) data appear to fall below the Hays data in Figures 3 through 5. This systematic error may indicate that the effective value of c for the larger depths of burial at Fort Sumner is higher than the average value of c for large depths at Hays. The Hays and Fort Sumner results do appear as parallel lines with a small offset. This observation indicates that a constant such as c and even the less probable ρ_g or g would improve the scatter were they known and inserted into the independent π term.

Additional evidence that h/d has an influence, but a very small one, on true crater size in the camouflet mode is presented in Figures 14 and 15 where normalized camouflet maximum radius and volume are plotted as functions of $W^{7/24}/d$ for data from Reference 3, which has no confining pavement. Figures 14 and 15 compare unconstrained camouflet data to the least-squares curve-fitted lines and their standard deviations from, respectively, Figure 11 for true maximum camouflet radius and Figure 13 for

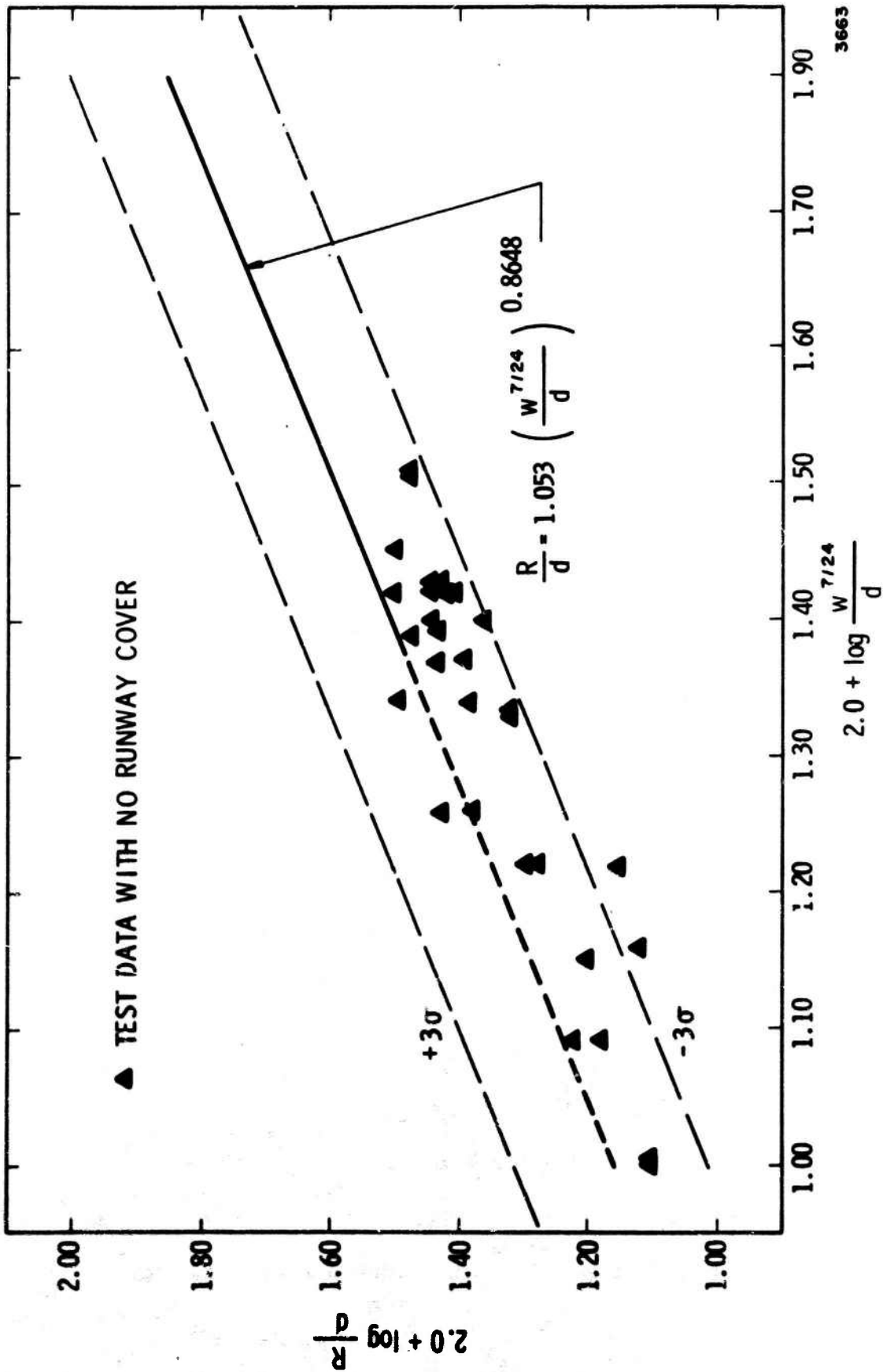


Figure 14. Normalized Camouflet Radius Without Pavement

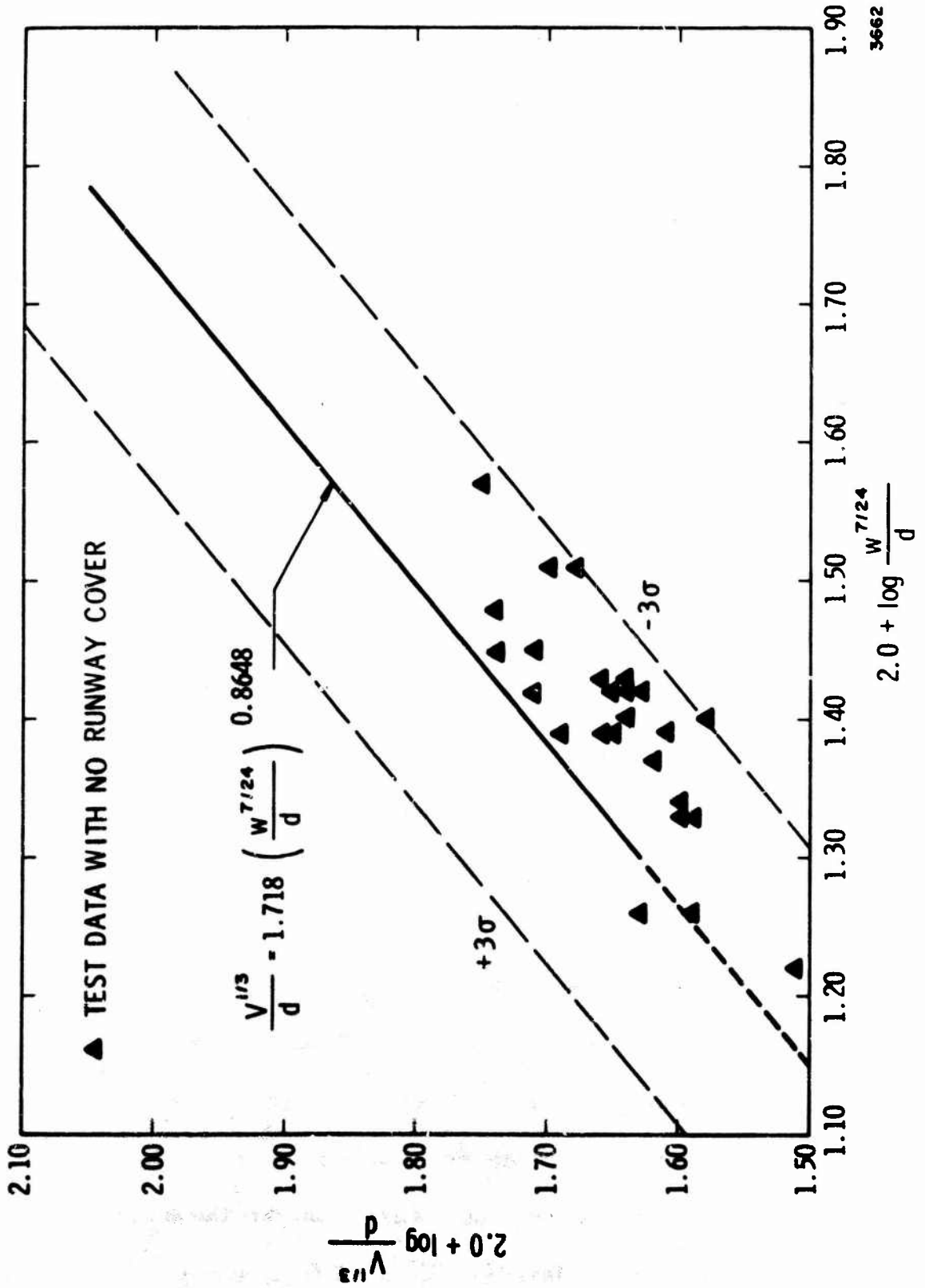
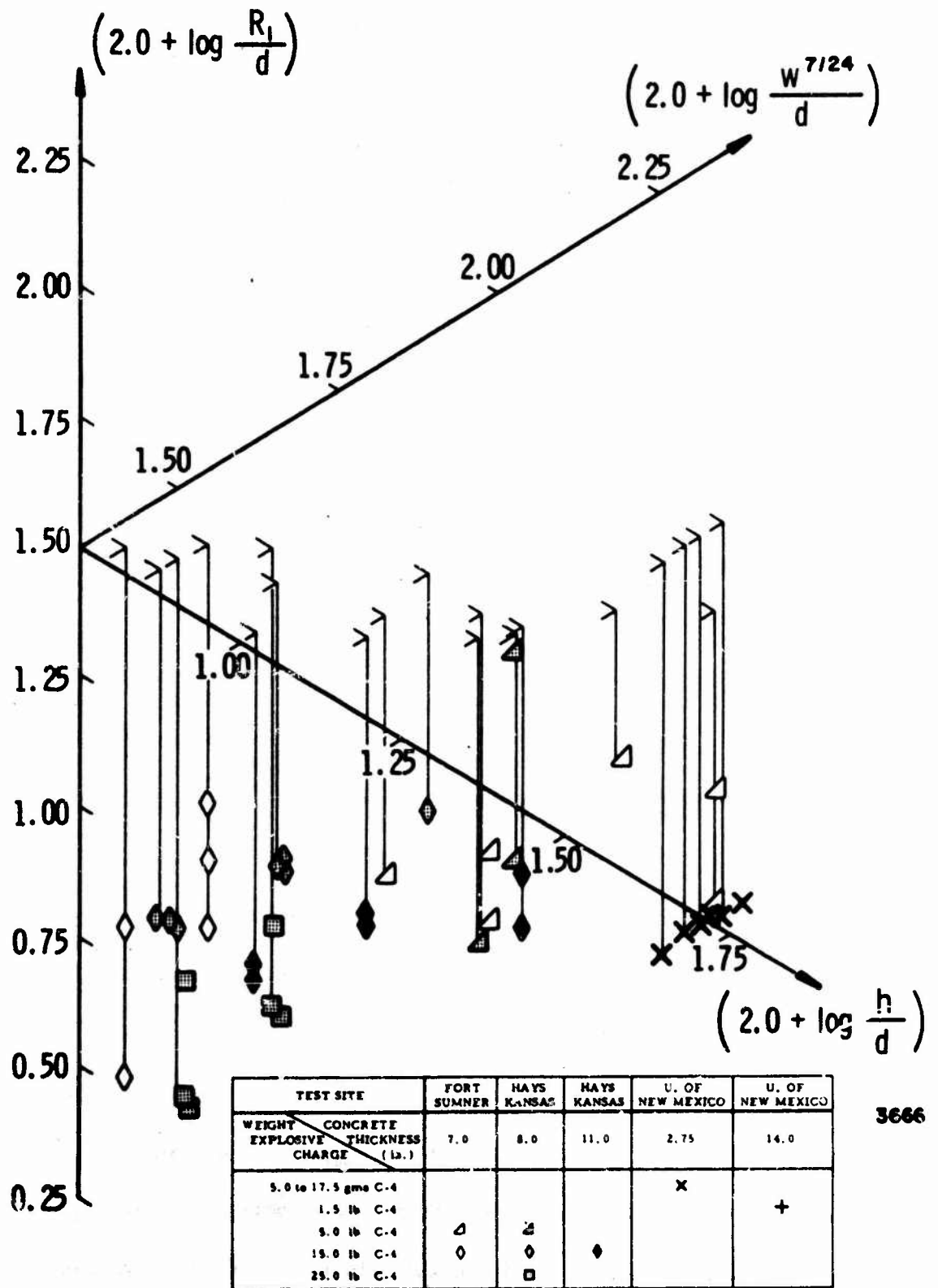


Figure 15. Normalized Camouflet Volume Without Pavement

soil and concrete volume. Because much of the data in Reference 3 are at even greater scaled depths of burial than the camouflet data for pavements in Reference 1, the lines which were curve-fitted must be extended. The dashed lines in Figures 14 and 15 are extensions to the curve-fitted lines. All unconstrained data lie close to the line and its extension especially when one considers the width of the three standard deviation confidence band; however, the unconfined data does fall below the runway camouflet line. This observation implies that h/d has some influence on true crater dimensions in the camouflet mode, but this influence is small. Nothing about similitude theory implies that the curve which we fit to data has to be straight. Because these additional data fall primarily in the lower left-hand corner of Figures 14 and 15, a curved relationship might be more appropriate and represent a more accurate curve-fit over a wider range in test results. The present straight-line relationships should only be applied for $W^{7/24}/d$ greater than 0.2.

Radius of crater at the surface of a camouflet and radius of concrete cracking are phenomena which can be influenced by surface conditions, especially concrete properties. Figure 16 is a three-dimensional graph of normalized surface crater radius in the camouflet mode as a function of normalized concrete thickness h/d and normalized energy release $W^{7/24}/d$. Two-dimensional



3666

Figure 16. Normalized Surface Crater Radius in Camouflet Mode

graphs of R_1/d as a function of $W^{7/24}/d$ exhibit enough extra scatter to imply that scaled concrete thickness is indeed a significant parameter. The general graphical solution to a relationship as shown in Figure 16 would be a surface over and through the h/d versus $W^{7/24}/d$ plane. Because most of the experimental data points were taken within a narrow band on the h/d versus $W^{7/24}/d$ plane, Figure 16 presents essentially one line from among the infinite number of lines defining the surface which is a solution for R_1/d as a function of h/d and $W^{7/24}/d$. Figure 16 can be used to graphically predict surface crater radius in the camouflet mode provided h/d and $W^{7/24}/d$ are related, as in Figure 16. If, for example, $W^{7/24}/d$ equaled 1.95 and h/d equaled 0.75, no prediction could be made of R_1/d because experimental data have not been obtained to define the surface which is the solution in this regime. Because Figure 16 verifies the modeling, but does not present a complete solution, no equation can be given for predicting R_1/d and no standard deviation can be calculated as an indication of accuracy.

The other surface parameter R_2/d probably is not a function of h/d , but it may be a function of $\sigma_{ult}/\rho_s c^2$ as in the cratering mode. Figure 17 presents radius of concrete cracking data as a function of $W^{7/24}/d$ for all values of h/d (h/d values in these experiments actually range from 0.06 to 0.46). Large

difference in charge weight are not given by the data in Figure 17; however, Fort Sumner and Hays data which have essentially the same value of σ_{ult} both appear to yield the same solution. The University of New Mexico modeling experiments appear to overestimate R_2/d in the camouflet mode. Remember this same group of experiments also overestimates R_2/d in the cratering mode, but σ_{ult} is significantly lower in the model tests than in the Fort Sumner and Hays experiments. A concrete which was weaker than desired would result in greater radii of concrete cracking. Rather insufficient quantities of model data are shown in Figure 17, only three data points, so whether or not R_2/d is also a function of σ_{ult} / ρ_c^2 cannot conclusively be determined without additional tests. An equation has been fitted to all the data except the model data in Figure 17. This relationship which is given by the following equation should only be used provided that σ_{ult} equals approximately 10,200 psi.

$$\frac{R_2}{d} = 6.421 \left(\frac{W}{d} \right)^{1.270} \quad \text{provided } \sigma_{ult} = 10,200 \text{ psi} \quad (13)$$

One standard deviation for Equation (13) equals 11.1% so R_2/d in the camouflet mode can be predicted with as great if not greater accuracy than R_2/d in the cratering mode. Distance between joints in concrete slabs and quantities of reinforcing are not scaled for the data in Figure 17, just as these quantities are not scaled

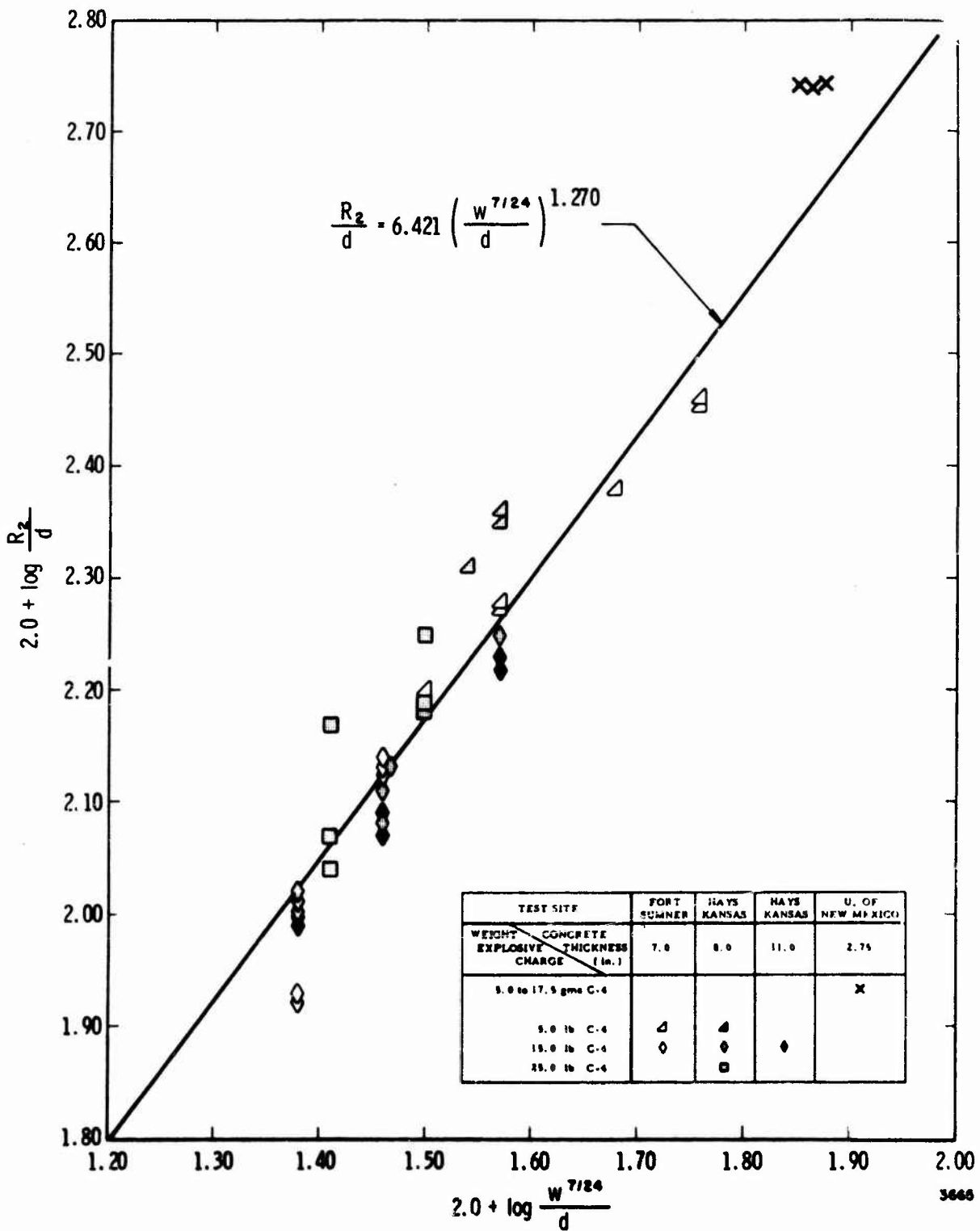


Figure 17. Normalized Radius of Concrete Cracking in Camouflet Mode

in the cratering mode. Apparently the appropriate magnitude of damage can be established even though these quantities are distorted.

We have not studied $V_1^{1/3}/d$ in the camouflet mode because V_1 essentially equals V_2 in the camouflet mode. Only a very small additional volume of concrete is added to the soil volume in a camouflet. Hence, in this mode, we do not study $V_1^{1/3}/d$, just as in the cratering mode we do not study R_3/d . Neither lends additional insight to this analysis.

SECTION VI
FABRICATING MODELS

The principle behind similitude theory is that individual variables do not have to be invariant; instead, if nondimensional ratios of products and quotients, called pi terms, remain invariant, different systems are equivalent. In this model analysis, we consider the parameters listed in Table V. These parameters do not have to be numerically equal in a different system. Provided that the independent pi terms listed in Table VII are equal in different systems, the dependent response pi terms listed in Table VII will be equal. Our major difficulty in designing a model experiment, which uses the same soils, same explosive, and tests in a 1-g gravitational environment as exists here on earth, is that with these constraints pi terms 4 and 5 from Table VII cannot be simultaneously satisfied.

If we are to use a physically smaller model experiment for predicting true crater size and the extent of cracking in a prototype runway system, then some length ratio λ will be assigned to our characteristic length, depth of burial d . Adopting the convention that:

$$\left(\quad \right)_r = \frac{\left(\quad \right) \text{ model}}{\left(\quad \right) \text{ prototype}}$$

where any parameter can be inserted into the brackets, similitude

requirements are imposed if we use the same materials in a smaller model here on earth in a 1-g gravitational field. These requirements are:

$$d_r = \lambda$$

$$\left(\frac{o}{s} \right)_r = 1.0$$

$$\left(\frac{\rho}{c} \right)_r = 1.0$$

$$\left(\frac{\sigma}{\text{ult}} \right)_r = 1.0$$

$$c_r = 1.0$$

$$g_r = 1.0$$

Pi terms 2 and 3 in Table VII are automatically satisfied by the proceeding requirements. Pi term 1 will be satisfied if we maintain geometric similarity and the h_r ratio equals λ . Difficulties arise because we cannot simultaneously scale W by λ^4 as required by pi term 4 and as λ^3 as required by pi term 5. We cannot build a model to a smaller scale, using the same materials and in a 1-g gravitational field, which satisfies a completely general model as presented in Equation (1) or its simplified version, Equation (2). We can only build models satisfying approximate versions of Equation (1) or must seek other model building techniques.

If we first determine the mode of response, a model can be fabricated. The same materials could be used in smaller model systems within the earth's natural gravitational field provided

charge weight W is scaled as λ^3 in the cratering mode and as $\lambda^{24/7}$ in the camouflet mode. Scaling charge weights in these manners would satisfy all responses if our evaluation of the model analysis is correct as presented in the preceding section. The necessity of scaling concrete strength and maintaining geometric similarity in the thickness of runways could probably be ignored if crater geometry only was studied; however, being more precise and satisfying these additional conditions should present no difficulties, so we recommend scaling concrete strength and maintaining geometric similarity in pavement thickness.

To create a model concrete, one might prefer using pea gravel or other small stone in place of a prototype large aggregate. In addition, the size of reinforcing rods should also be scaled so that steel does not provide a disproportionate amount of strength in the model. These actions will require other cement-to-water ratios in a model concrete because the surface areas being wetted are no longer scaled unless the grain size of sand and cement are also scaled, a very difficult and impractical undertaking. Several trial mixes should lead to a concrete with the appropriate strength. We have indicated that models do not necessarily have to model concrete strength; however, we would point out that all data to date have been taken within a narrow band on the mode shape curve of $W^{1/4}/d$ versus $W^{1/3}/d$, Figure 2. Experiments conducted

outside this band could well result in pi terms such as h/d and $\sigma_{ult} / \rho_s c^2$ becoming significant. Any observations in the preceding section can only be said to rigorously apply for tests within the experimental band shown in Figure 2.

Under some circumstances, model tests cannot be conducted in the cratering mode, although we believe they are always possible in the camouflet mode. As an example of why a model test might be impossible in the cratering mode, consider the following illustration. Assume that one wishes to build a 1/5 scale model to determine true crater size for a prototype 194.4-pound charge buried 16.3 feet deep. The quantity $(2.0 + \log W^{1/3}/d)$ equals 1.55 and $(2.0 + \log W^{1/4}/d)$ equals 1.36 which indicate in Figure 2 that the response is just within the cratering mode. If the response is in the cratering mode, we should scale W as λ^3 , and our 1/5 scale model yields a charge weight of 1.555 pounds at a depth of 3.26 feet. Before testing our model, we should check its mode of response. The model quantity $(2.0 + \log W^{1/3}/d)$ equals 1.55 as does the prototype, but the quantity $(2.0 + \log W^{1/4}/d)$ equals 1.535. Figure 2 indicates that the response of the model falls in the camouflet mode, so we would not obtain the proper results in a model experiment. This example demonstrates that a model experiment can change modes from the cratering to the camouflet mode. We have not been able to devise a set of circumstances in

which a model would be in the cratering mode when the prototype was in the camouflet mode. Generally model points fall above corresponding prototype points and sometimes to the left of them as shown in Figure 2; hence, it is difficult to slip from the camouflet into the cratering mode.

One method does exist for satisfying all pi terms in Equation (1); however, very special equipment is required. If one has access to a centrifuge, an artificial body force can be generated which approximates the influences of gravity on a bed of soil. All pi terms in Equation (1) will be satisfied if the charge weight W is scaled as λ^3 and the acceleration of gravity is scaled as $1/\lambda$. Because the factor $1/\lambda$ will be greater than one, this technique will theoretically work. The weakness in this approach is that the larger the scale factor, the longer the arms on the centrifuge and the higher the angular velocity. In addition, people having centrifuges are generally reluctant to have explosives threatening their apparatus.

By way of a review, Table X has been compiled to summarize how each parameter will usually be scaled. The mode of response must be checked for both model and prototype conditions. If both model and prototype systems fall within the same mode of response, the scale factors presented in Table X should work fairly well. Notice only the charge weight is scaled differently in various modes.

Table X

SCALE FACTORS FOR MODEL CRATERING EXPERIMENTS

<u>Parameter</u>	<u>Symbol</u>	<u>Scale Factor In Cratering Mode</u>	<u>Scale Factor In Camouflet Mode</u>
Depth Burial	d	λ	λ
Thickness of Concrete	h	λ	λ
Density of Concrete	ρ_c	1.0	1.0
Ultimate Strength of Concrete	σ_{ult}	1.0	1.0
Acceleration of Gravity	g	Not Scaled	1.0
Density of Soil	ρ_s	1.0	1.0
Seismic Velocity of Soil	c	1.0	1.0
Charge Weight	W	λ^3	$\lambda^{24/7}$
Volume of Crater	V	λ^3	λ^3
Depth of Crater	D	λ	λ
Radius of Crater or of Concrete Cracking	R	λ	λ

SECTION VII
RECOMMENDATIONS FOR FUTURE EXPERIMENTS

If additional experimental bomb cratering data are to be obtained either with model or full-scale experiments, we recommend investigating three specific subjects and perhaps two more which would be of interest. Figure 2, our plot of $W^{1/4}/d$ versus $W^{1/3}/d$, giving the mode of response shows that all data were taken within a very narrow band relating charge weight and depth of burial. All conclusions are based upon data from within this band of charge weight and depth of burial. The question should naturally arise as to what happens outside the band. Charge weight and depth of burial conditions were picked because experimenters were seeking conditions which maximized damage; however, if a more general solution is desired, the experimental space being investigated should be covered more thoroughly. We have assumed that many phenomena are relatively insignificant and have used data from within a narrow band of conditions to substantiate these conclusions. Additional data outside the band of initial conditions might demonstrate that effects felt to be insignificant do indeed matter under other conditions.

As a first priority, we recommend establishing the curve separating the cratering and camouflet modes over a wider range

in initial conditions. Figure 2 and the equation associated with it should presently be used only for values of $(2.0 + \log W^{1/3}/d)$ between 1.55 and 1.82, values of $W^{1/3}/d$ between 0.355 and 0.661. This line separating modes of response goes somewhere which remains to be determined outside this narrow range. If a cratering condition falls in a region where the mode of response is not known, predictions cannot be made. Additional cratering data would not only establish mode of response more accurately but also provide additional data on magnitude of responses.

As a second priority, we strongly recommend collecting additional data in the camouflet mode. Absolutely no experiments using bombs were conducted in this regime, and the few model tests that were performed using gram charges have many critics skeptical of the results. The vast majority of data which everyone appears prepared to accept involves energy releases between 5 and 25 pounds of C-4. Our conclusions in the camouflet mode must be accepted as tentative because a factor of 5 difference in charge weight only represents a very small 60% variation in the important independent variable $W^{7/24}$. A few experiments using 750-pound bombs in the camouflet mode would be expensive; however, they would increase this very small 60% variation in $W^{7/24}$ to a much more significant 402% variation. Supplement four to five bomb tests with additional model experiments having

charges less than a pound and the analysis in the camouflet mode would either be on more solid grounds or would be modified.

As a third priority, we recommend model experiments to determine the influence of concrete strength on surface-related responses in both the cratering and camouflet modes. The vast majority of experiments which were conducted at Fort Sumner and Hays all had concretes with essentially the same ultimate compressive strength of 10,200 psi. Cracking of concrete in both modes and radius of surface crater in the camouflet mode are responses which appear to have a dependency on concrete strength. Until additional test results are acquired, inadequate amounts of information exist to empirically determine how the pi term $\sigma_{ult} / \rho_s c^2$ influences R_1/d in the camouflet mode and especially R_2/d in both the camouflet and cratering modes.

Recommendations of lower priority, but which could be easily accomplished, include measuring the seismic velocity as a function of depth at the Fort Sumner and Hays test sites and conducting more experiments to simulate bombs up in the concrete. If the seismic velocity c were accurately known as a function of depth, an averaging procedure might be developed for obtaining an effective seismic velocity c_{eff} which could reduce scatter. Provided moisture contents were much the same under the pavements at Fort Sumner and Hays, measurements of c taken

now should not differ too greatly from the actual value of c at the time of testing.

Only seven tests were conducted with the center of charges in the concrete. This experimental condition does lend itself to model tests, so if information is desired on cratering from charges within the pavement or even because of surface burst, we recommend using models. Scaled thickness of concrete h/d and scaled concrete strength $\sigma_{ult} / \rho_s c^2$ would probably become significant parameters, and would certainly be important parameters for air bursts.

If additional tests as recommended herein were conducted, the general overall need to obtain some response data outside the band on the $W^{1/4}/d$ versus $W^{1/3}/d$ plot would be met. Essentially our recommendations acknowledge that additional experimental data could be beneficially utilized. We are attempting in these recommendations to direct any additional experiments which might be conducted towards specific objectives which, when addressed, will provide the most additional insight into bomb cratering of runways.

SECTION VIII

SUMMARY

In this report, a model analysis is conducted and procedures are recommended for using small scale experiments to determine the extent of bomb crater damage to rigid runways. Empirical formulae were also devised for estimating true crater size and the extent of concrete cracking. Before one can decide how charge weight should be scaled in a model or what empirical formula applies for predicting true crater size, one must determine if the mode of response falls in the camouflet or cratering mode. Different physical phenomena are important in the two different response modes. Gravitational effects are significant in the camouflet mode, but not in the cratering mode. Concrete pavement strength and thickness play essentially no role in the cratering mode except perhaps for radius of concrete cracking; however, they influence surface phenomena such as surface crater radius and extent of cracking in the camouflet mode. One refers to a plot of $W^{1/4}/d$ versus $W^{1/3}/d$ where W is charge weight and d is depth of burial to determine whether the cratering or camouflet mode predominates. If the value of $W^{1/4}/d$ to be tested is greater than the calculated value of $W^{1/4}/d$ from Equation (4),*

* Equations in this summary are numbered as in the text.

the response falls in the camouflet mode, and if this value is less, it falls in the cratering mode.

$$(2.0 + \log \frac{W^{1/4}}{d}) = 1.3981 (2.0 + \log \frac{W^{1/3}}{d}) \tanh^5 (2.0 + \log \frac{W^{1/3}}{d}) \quad (4)$$

In the cratering mode, a replica modeling law is appropriate, and charge weight scales as the geometric scale factor cubed.

Experimental data indicate that the presence of the pavement has an insignificant influence on true crater size. Empirical equations obtained by curve-fitting least squares straight lines to nondimensional pi terms from a similitude analysis yield Equation (5) for predicting true surface crater radius, Equation (6) for predicting true crater depth, Equation (7) for predicting true soil crater volume, and Equation (8) for predicting soil plus concrete crater volume. One standard deviation calculated from

$$\frac{R_1}{d} = 2.155 \left(\frac{W^{1/3}}{d} \right)^{0.865} \quad (5)$$

$$\frac{D}{d} = 2.312 \left(\frac{W^{1/3}}{d} \right)^{0.6833} \quad (6)$$

$$\frac{V_1}{d} = 2.046 \left(\frac{W^{1/3}}{d} \right)^{0.7849} \quad (7)$$

$$\frac{V_2}{d} = 2.372 \left(\frac{W^{1/3}}{d} \right)^{0.8227} \quad (8)$$

experimental data equals essentially 12% for all normalized dependent variables except R_1/d where the standard deviation equals approximately 20%. Although the author believes this accuracy is excellent, ideas are suggested which, if followed, might improve the accuracy moderately. Radius of concrete cracking in the cratering mode can be estimated using Equation (9) provided the ultimate strength of the concrete is approximately 10,200 psi.

$$\frac{R_2}{d} = 4.247 \left(\frac{W}{d} \right)^{1/3} \cdot 0.9831 \quad (9)$$

The amount of cracking probably depends to a moderate amount on scaled concrete strength, but not on scaled depths of burial. Because most of the data are on concrete pavements with strength of 10,200 psi, empirical formulae could not be devised for other strength concretes in the cratering modes. Unless concrete strength cause changes in mode of failure or energy transfer mechanisms, higher strength concretes probably crack less and weaker strength concretes probably crack more than estimated using Equation (9).

In the camouflet mode, an empirically obtained compromise coefficient is used to scale charge weight as the geometric scale factor to the 7/24 power. This coefficient is a compromise between the one fourth power associated with scaling gravitational and inertial effects and the one third power associated with scaling

strength or constitutive and inertial effects. Empirical equations for predicting crater size in the camouflet mode have been developed from least-squares fits to straight lines on log-log plots of nondimensional pi terms. Equation (10) is for predicting maximum crater radius, Equation (11) is for predicting true crater depth, and Equation 12 is for predicting true crater volume.

$$\frac{R_3}{d} = 1.053 \left(\frac{W}{d} \right)^{0.8648} \quad (10)$$

$$\frac{D}{d} = 2.244 \left(\frac{W}{d} \right)^{0.4324} \quad (11)$$

$$\frac{V_2^{1/3}}{d} = 1.718 \left(\frac{W}{d} \right)^{0.8648} \quad (12)$$

One standard deviation was predicted for these curves and equaled approximately 12%. Because the range in charge weight is nowhere as large in the camouflet mode as in the cratering mode, this low standard deviation is not as significant. Radius of concrete cracking in the camouflet mode can also be estimated provided that the strength of the concrete is approximately 10,200 psi. Equation (13) is the equation for predicting radius of cracking.

$$\frac{R_2}{d} = 6.421 \left(\frac{W}{d} \right)^{1.270} \quad (13)$$

One standard deviation for R_2/d equals 11% even though scaled thickness of concrete and scaled slab dimensions are not considered in this analysis.

This report closes with a list of five recommendations for future experiments. We suggest that additional data be obtained to: 1) establish the curve separating the cratering and camouflet modes over a wider range in initial conditions, 2) measure true crater size over a wider range of charge weights in the camouflet mode, 3) study the influence of concrete strength on surface related phenomena in both response modes, 4) determine the influence of soil strength especially the seismic velocity of the soil on crater size, and 5) evaluate the effects on bomb detonation inside the pavement on crater geometry and concrete cracking. We believe much additional valuable data can be obtained using model experiments.

REFERENCES

1. Asbjorn Kvammen, Jr., Raman Pichumani, and James L. Dick, Jr., Pavement Cratering Studies, University of New Mexico, Eric H. Wang Research Facility report for Air Force Weapons Laboratory, Kirtland Air Force Base, (In Preparation).
2. W. R. Tomlinson, Jr. and O. E. Sheffield, Engineering Design Handbook, Explosions Series, Properties of Explosives of Military Interest, AMC Pamphlet 706-177, Headquarters, U. S. Army Materiel Command, March 1967.
3. R. A. Sager, C. W. Denzel, and W. B. Tiffany, Cratering From High Explosive Charges, Compendium of Crater Data, Waterways Experiment Station Technical Report No. 2-547, Report 1, Vicksburg, Mississippi, May 1960.
4. P. S. Westine, "Explosive Cratering," Journal of Terra-mechanics, VII, 2, 1970, pp. 9-19.

UNCLASSIFIED

Security Classification

DOCUMENT CONTROL DATA - R & D

(Security classification of title, body of abstract and indexing annotation must be entered when the overall report is classified)

1. ORIGINATING ACTIVITY (Corporate author) Southwest Research Institute 8500 Culebra Road San Antonio, Texas 78228		2a. REPORT SECURITY CLASSIFICATION UNCLASSIFIED	
		2b. GROUP	
3. REPORT TITLE BOMB CRATER DAMAGE TO RUNWAYS			
4. DESCRIPTIVE NOTES (Type of report and inclusive dates) February 1972 through November 1972			
5. AUTHOR(S) (First name, middle initial, last name) Peter S. Westine			
6. REPORT DATE February 1973		7a. TOTAL NO. OF PAGES 88	7b. NO. OF REFS 4
8a. CONTRACT OR GRANT NO. F29601-72-C-0053		9a. ORIGINATOR'S REPORT NUMBER(S) AFWL-TR-72-183	
b. PROJECT NO. 683M		9b. OTHER REPORT NO(S) (Any other numbers that may be assigned this report)	
c.			
d.			
10. DISTRIBUTION STATEMENT Distribution limited to US Government agencies only because of test and evaluation (15 Jan 73). Other requests for this document must be referred to AFWL (DEZ), Kirtland AFB, NM 87117.			
11. SUPPLEMENTARY NOTES		12. SPONSORING MILITARY ACTIVITY AFWL (DE) Kirtland AFB, NM 87117	
13. ABSTRACT (Distribution Limitation Statement B) A similitude analysis is conducted and procedures are presented for using model tests to determine the extent of bomb crater damage to rigid runways. The radius, depth, and volume of true craters, as well as the extent of concrete cracking, can all be determined; however, different methods to scale the energy release are required, dependent upon a crater or camouflet being formed. Experimental test data using energy releases ranging from 5 grams to 589 pounds (750-pound bomb) of C-4 are used to demonstrate the validity of this model analysis. In addition, empirical equations have been curve-fitted to the pi terms and can be used for predicting mode of response, true crater size, and extent of concrete cracking.			

UNCLASSIFIED

Security Classification

14. KEY WORDS	LINK A		LINK B		LINK C	
	ROLE	WT	ROLE	WT	ROLE	WT
Cratering Bomb damage Runways Explosive cratering True crater						

UNCLASSIFIED

Security Classification